Neo-formation of chromosomes in bacteria.

Olivier Poirion, Bénédicte Lafay

Neo-formation of chromosomes in bacteria

Olivier B. Poirion[1,2†] & Bénédicte Lafay[1,2,3*]

[1] Université de Lyon, F-69134 Lyon, France

[2] CNRS (French National Center for Scientific Research) UMR5005, Laboratoire Ampère, École Centrale de Lyon, 36 avenue Guy de Collongue, 69134 Écully, France

[3] CNRS (French National Center for Scientific Research) UMR5558, Laboratoire de Biométrie et Biologie Évolutive, Université Claude Bernard – Lyon 1, 43 boulevard du 11 novembre 1918, 69622 Villeurbanne cedex, France

[†] Current address: Center for Epigenomics, Department of Cellular and Molecular Medicine, University of California, San Diego, School of Medicine, 9500 Gilman Drive, La Jolla, CA 92093, USA

* Author for correspondence: benedicte.lafay@univ-lyon1.fr

ABSTRACT

Although the bacterial secondary chromosomes/megaplasmids/chromids, first noticed about forty years ago, are commonly held to originate from stabilized plasmids, their true nature and definition are yet to be resolved. On the premise that the integration of a replicon within the cell cycle is key to deciphering its essential nature, we show that the content in genes involved in the replication, partition and segregation of the replicons and in the cell cycle discriminates the bacterial replicons into chromosomes, plasmids, and another class of essential genomic elements that function as chromosomes. These latter do not derive directly from plasmids. Rather, they arise from the fission of a multi-replicon molecule corresponding to the co-integrated and rearranged ancestral chromosome and plasmid. All essential replicons in a distributed genome are thus neo-chromosomes. Having a distributed genome appears to extend and accelerate the exploration of the bacterial genome evolutionary landscape, producing complex regulation and leading to novel eco-phenotypes and species diversification.

INTRODUCTION

Chromosomes are the only components of the genome that encode the necessary information for replication and life of the cell/organism under normal growth conditions. Their number varies across taxa, a single chromosome being the standard in bacteria (Krawiec and Riley, 1990). Evidence accumulated over the past forty years is proving otherwise: bacterial genomes can be distributed on more than one chromosome-like autonomously replicating genomic element (replicon) (Casjens, 1998; diCenzo and Finan, 2017; Mackenzie et al., 2004). The largest, primary, essential replicon (ER) in a multipartite genome corresponds to a *bona fide* chromosome and the additional, secondary, ERs (SERs) are expected to derive from accessory replicons (plasmids (Lederberg, 1998)). The most popular model of SER formation posits that a plasmid acquired by a mono-chromosome progenitor bacterium is stabilized in the genome through the transfer from the chromosome of genes essential to the cell viability (diCenzo and Finan, 2017; diCenzo et al., 2013; Slater et al., 2009). The existence in SERs of plasmid-like replication and partition systems (Dubarry et al., 2006; Egan and Waldor, 2003; Livny et al., 2007; MacLellan et al., 2004, 2006; Slater et al., 2009; Yamaichi et al., 2007) as well as experimental results (diCenzo et al., 2014) support this view. Yet, the duplication and maintenance processes of SERs contrast with the typical behaviour of plasmids for which both the timing of replication initiation and the centromere movement are random (Million-Weaver and Camps, 2014; Reyes-Lamothe et al., 2014). Indeed, the SERs share many characteristic features with chromosomes: enrichment in Dam methylation sites of the replication origin (Egan and Waldor, 2003; Gerding et al., 2015), presence of initiator titration sites (Egan and Waldor, 2003; Venkova-Canova and Chattoraj, 2011), synchronization of the replication with the cell cycle (De Nisco et al., 2014; Deghelt et al., 2014; Egan and Waldor, 2003; Egan et al.,

2004; Fiebig et al., 2006; Frage et al., 2016; Kahng and Shapiro, 2003; Rasmussen et al., 2007; Srivastava et al., 2006; Stokke et al., 2011), KOPS-guided FtsK translocation (Val et al., 2008), FtsK-dependent dimer resolution system (Val et al., 2008), MatP/matS macrodomain organisation system (Demarre et al., 2014), and similar fine-scale segregation dynamics (Fiebig et al., 2006; Frage et al., 2016). Within a multipartite genome, the replication of the chromosome and that of the SER(s) are initiated at different time points (De Nisco et al., 2014; Deghelt et al., 2014; Fiebig et al., 2006; Frage et al., 2016; Rasmussen et al., 2007; Srivastava et al., 2006; Stokke et al., 2011), and use replicon-specific systems (Drevinek et al., 2008; Egan and Waldor, 2003; Galardini et al., 2013; MacLellan et al., 2004, 2006; Slater et al., 2009). Yet, they are coordinated, hence maintaining the genome stoichiometry (Deghelt et al., 2014; Egan et al., 2004; Fiebig et al., 2006; Frage et al., 2016; Stokke et al., 2011). In the few species where this was studied, the replication of the SER is initiated after that of the chromosome (De Nisco et al., 2014; Deghelt et al., 2014; Fiebig et al., 2006; Frage et al., 2016; Rasmussen et al., 2007; Srivastava, 2006; Stokke et al., 2011) under various modalities. In the Vibrionaceae, the replication of a short region of the chromosome licenses the SER duplication (Baek and Chattoraj, 2014; Kemter et al., 2018), and the advancement of the SER replication and segregation triggers the divisome assembly (Galli et al., 2016). In turn, the altering of the chromosome replication does not affect the replication initiation control of the SER in α-proteobacterium *Ensifer/Sinorhizobium meliloti* (Frage et al., 2016).

Beside the exploration of the replication/segregation mechanistic, studies of multipartite genomes, targeting a single bacterial species or genus (diCenzo et al., 2013, 2014; Dubarry et al., 2006; Mackenzie et al., 2004; Slater et al., 2009) or using a more extensive set of taxa (diCenzo and Finan, 2017; Harrison et al., 2010), relied on

77 inadequate (replicon size, nucleotide composition, coding of core essential genes for
78 growth and survival (diCenzo and Finan, 2017; Harrison et al., 2010; Liu et al., 2015);
79 Figure 1) and/or oriented (presence of plasmid-type systems for genome maintenance
80 and replication initiation (Harrison et al., 2010)) criteria to characterize the SERs.

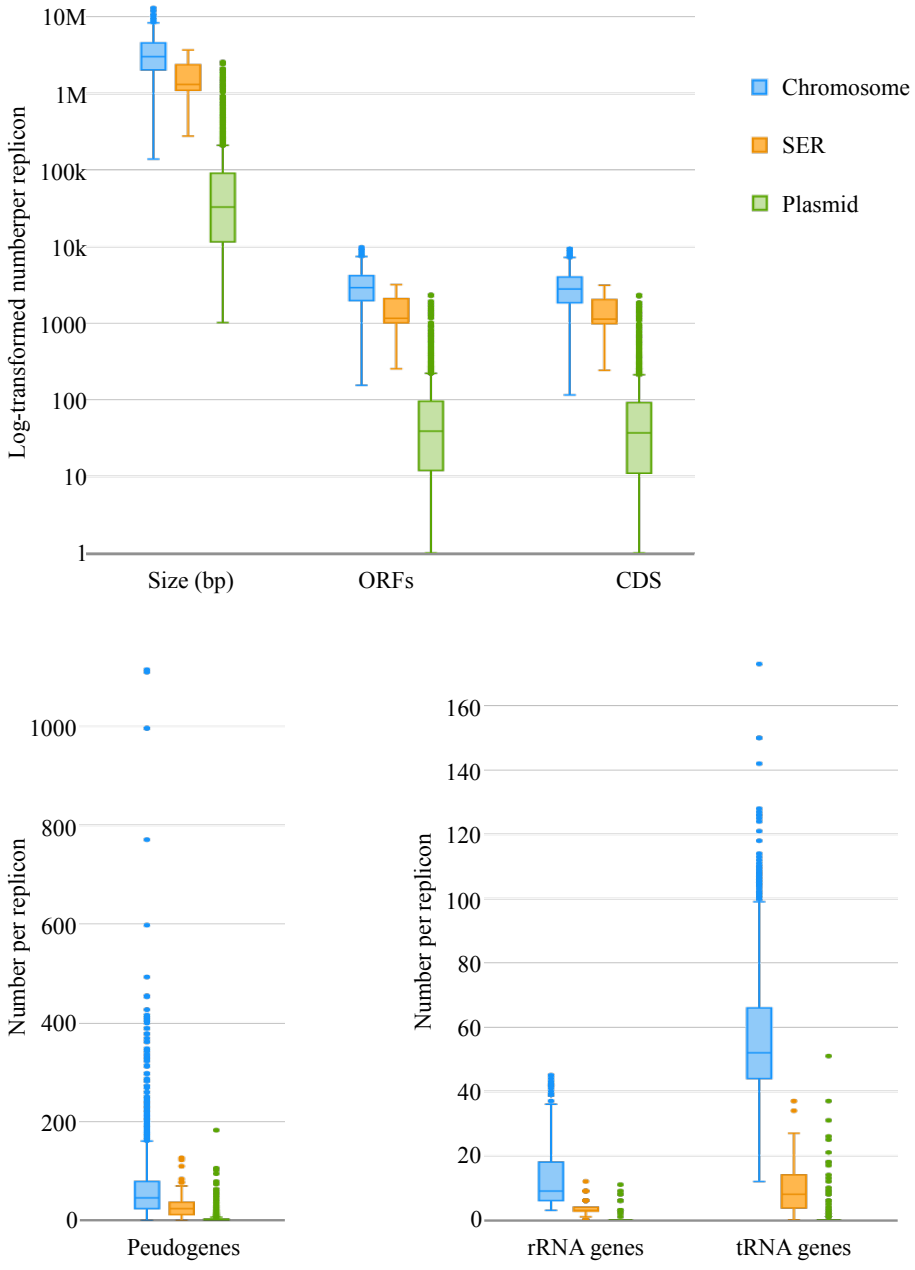

81

82 **Figure 1. Structural features of the replicons**

83 Boxplots of the lengths (base pairs) and numbers of genes (ORFs), protein-coding genes (CDS), pseudogenes,
84 ribosomal RNA genes and transfer RNA genes for the 2016 chromosomes (blue), 129 SERs (orange), and 2783
85 plasmids (green) included in the final dataset (4928 replicons).

While clarifying the functional and evolutionary contributions of each type of replicon to a multipartite genome in given bacterial lineages (Galardini et al., 2013; Harrison et al., 2010; MacLellan et al., 2004; Slater et al., 2009), these studies produced no absolute definition of SERs (diCenzo and Finan, 2017; Harrison et al., 2010) or universal model for their emergence (diCenzo and Finan, 2017; diCenzo et al., 2013, 2014; Galardini et al., 2013; Harrison et al., 2010). We thus set out investigating the nature(s) and origin(s) of these replicons using as few assumptions as possible.

RESULTS

Replicon inheritance systems as diagnostic features

We did not limit our study to a particular multipartite genome or a unique gene family. Rather, we performed a global analysis encompassing all bacterial replicons whose complete sequence was available in public sequence databases (Figure 2). We reasoned that the key property discriminating the chromosomes from the plasmids is their transmission from mother to daughter cells during the bacterial cell cycle. The functions involved in the replication, partition and maintenance of a replicon, *i.e.*, its inheritance systems (ISs), thence are expected to reflect the replicon degree of integration into the host cycle.

We first faced the challenge of identifying all IS functional homologues. The inheritance of genetic information requires functionally diverse and heterogeneous actuators depending on the replicon type and the characteristics of the organism. Also, selecting sequence orthologues whilst avoiding false positives (*e.g.*, sequence paralogues) can be tricky since remote sequence homology most likely prevails among chromosome/plasmid protein-homologue pairs.

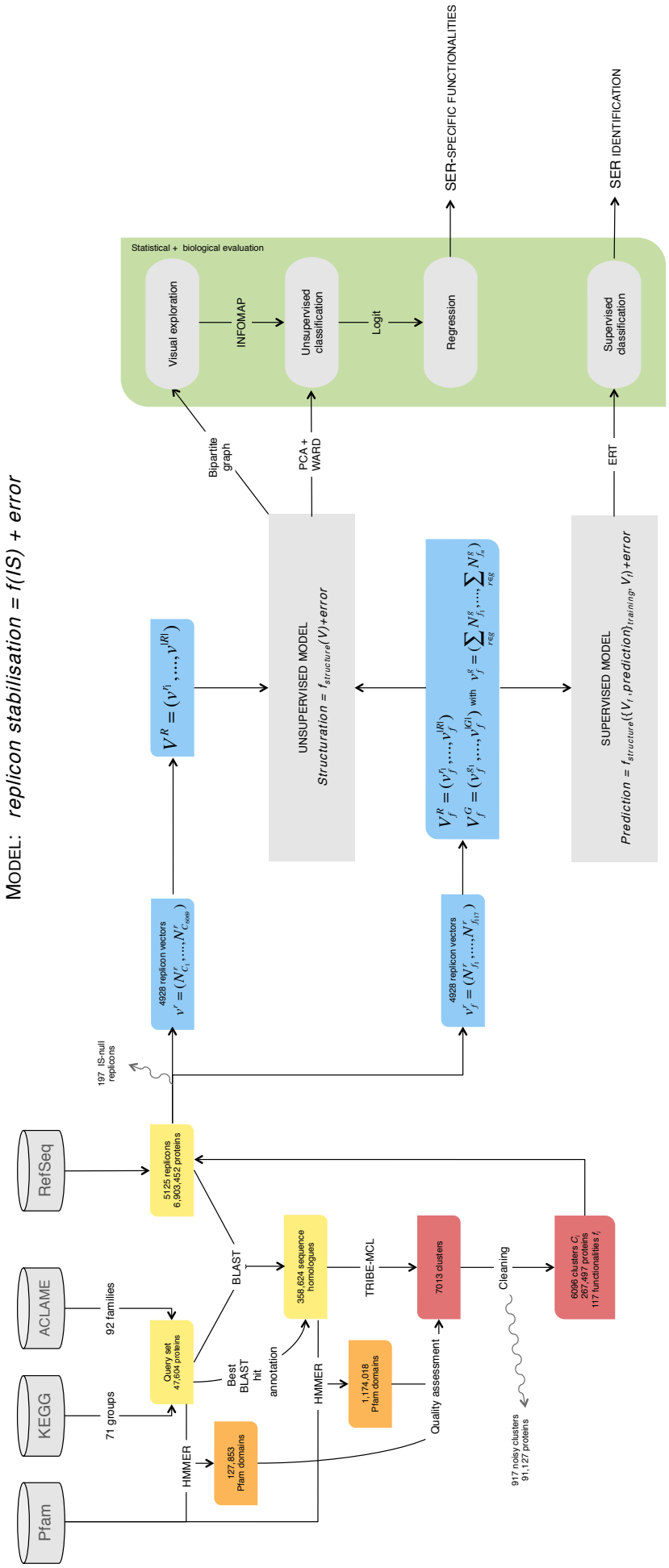

Figure 2. Analytical procedure

Starting from an initial dataset of 5125 replicons, we identified 358,624 putative IS functional homologues, overall corresponding to 1711 Pfam functional domains (Figure 3a), using a query set of 47,604 chromosomal and plasmidic IS-related proteins selected from the KEGG and ACLAME databases (Tables 1 and 2).

Table 1. ACLAME families used in the building of the query set

PROCESS	FAMILY	PROTEIN DESCRIPTION
Replication	*32*	RepB, pi, initiator protein, RepE, RepA
	76	Rep, RepB, Rep of rolling circle initiator, RepA, RepU, OrfB, Rep2
	107	RepC, RepCa1, RepCa2, RepCd
	114	Helicase, UrvD rep helicase, helicase super family 1, Yga2F, helicase II
	118	CdsE, CdsJ
	133	RepA, W0005, RepA1/A2
	171	RepA, RepB, putative theta replicative protein
	207	replicative DNA helicase, DnaB, pGP1
	208	RepA, W0013, W0041, RepFIB
	224	long form TrfA, TrfA1, TrfA2, S-TrfA, plasmid initiation protein
	237	RepA, putative RepA, truncated RepA
	244	RepA, RepB, CopB, repA1/A2, w0004
	294	Rop regulatory protein, RNAI modulator, RNA modulator, plasmid copy number control
	297	primase activity/DNA initiation, LtrC/LtrC-like hypothetical protein, PcfD
	330	DNA repair/ DNA helicase, type III restriction enzyme, res subunit, DEAD/DEAH box helicase
	377	replicase, replication initiation, RepC, RepJ, RepE, RepL
	383	RepA, Rb100
	404	RepA,RepB,RepW
	412	Rep, RepA
	423	truncated RCR replication, RepRC, RepB, OrfA
	426	cell division control protein 6 homolog
	440	Rep 14-4, rm protein, RepA hypothetical protein
	451	RepA, host type : *Corynebacterium*
	477	Rep, RepS, RepE, host type : *Bacillus*, RepS, RepR
	612	RepL, replication initiation
	775	DNA helicase activity, RepA, putative helicase
	854	DNA helicase activity, RepC, putative initiator protein
	921	RepA
	931	DNA replication initiation, putative protein, CdsD
	1005	helicase activity, putative protein, hypothetical helicase
	1055	RNA polymerase σ factor, σ 70 family, bacteriocin uviA, sigF/V/G, tetR, host type : *Clostridium*
	1095	DNA repair/helicase, RuvB, DNA pol III γ and τ subunits, DNA pol δ subunit
	1099	putative theta replicase, RepB, Rep2
	1187	DNA replication, RepH, RepI
	1288	RepA
	1345	DNA primase activity, DNA primase , primase CHC2 family
	1398	helicase activity, GcrE, GcrC

	1652	DNA repair/exonuclease activity, DNA exonuclease protein, SbcCD related protein
	1837	putative replication protein
	2881	RepC-like, Pif
Partition	*4*	plasmid partition protein, ParA, ParA IncC protein, ParA InC1/ IncC2, SopA, virC1
	14	RepB, RepB partitionning, KorB repressor and partitionning, ParB-like domain, YefA, YdeB, ParB, ParB-like
	102	DNA binding, partitionning protein, control protein, ParB, VirB, partition protein B
	128	DNA segregation/DNA translocase activity, cell division FtsK/ SpoIIIE, SpoI, TraB
	289	ParM family, go : translocase, hypothetical protein, rode shape protein, putative ATPase of class HSP70
	316	microfilament motor activity, ParM family, StbA protein, stable inheritance protein, ParA
	318	ATPase, regulation of cell division, chromosome patition, GumC, ExoP related protein, EpsB, MPA1 family
	427	ATPase family, ParR family, ParB, StbB, mediator of plasmid stability
	875	DNA binding, partitionning protein family ParB/Spo0J, YPMT1.28c
	876	DNA binding, partitionning protein family ParB/Spo0J, YPMT1.29c
	983	DNA binding, ParB, CopG
	1227	DNA plasmid copy number control, CopG
	2158	RepC
	2894	DNA binding
Dimer resolution	*5*	serine based recombinase activity, ylb, resolvase, second invertase, TniR, ParA
	10	tyrosine-based recombinase, integrase, putative integrase, Xer, recombinase-like SAM
	101	plasmid dimer resolution, tyrosine-based recombinase, yld, SAM-like protein
	170	tyrosine-based recombinase, OrfA, hypothetical protein
	589	tyrosine based protein, Fis protein
	688	tyrosine based protein, SAM like protein, XerD
Maintenance	*100*	Postsegregational killing system vapBC/vag
	136	Postsegregational killing system parDE
	156	Postsegregational killing system epsilon-zeta
	201	Postsegregational killing system higBA
	212	Postsegregational killing system parDE
	293	Postsegregational killing system mazEF
	319	Postsegregational killing system relBE
	326	Postsegregational killing system mazEF
	335	Postsegregational killing system HOK/SOK
	338	Postsegregational killing system parDE
	356	Postsegregational killing system parDE
	366	Postsegregational killing system vapBC/vag
	380	Postsegregational killing system phD-doc
	428	Postsegregational killing system ccd
	470	Postsegregational killing system yacA
	474	Postsegregational killing system relBE
	515	Postsegregational killing system relBE
	556	Postsegregational killing system higBA
	563	Postsegregational killing system ccd
	588	Postsegregational killing system higBA
	677	Postsegregational killing system higBA
	798	Postsegregational killing system mazEF
	916	Postsegregational killing system relBE
	1031	Postsegregational killing system HOK/SOK
	1180	Postsegregational killing system vapXD
	1308	Postsegregational killing system HicAB
	1559	Postsegregational killing system epsilon-zeta
	1927	Postsegregational killing system mazEF

	3357	Postsegregational killing system, plasmid maintenance
	4776	Postsegregational killing system, parC
	4777	Postsegregational killing system parDE, parD
	16584	Postsegregational killing system vapXD

Table 2. KEGG "Prokaryotic-type chromosome" orthology groups used in the building of the query set

BRITE HIERARCHY		KEGG ENTRY	NAME	DEFINITION
Chromosome replication	Initiation factors (bacterial)	*K02313*	DnaA	chromosomal replication initiator protein
		K02314	DnaB	replicative DNA helicase [EC:3.6.4.12]
		K03346	DnaB2, DnaB	replication initiation and membrane attachment protein
		K02315	DnaC	DNA replication factor, helicase loader
		K02316	DnaG	DNA primase [EC:2.7.7.-]
		K11144	DnaI	primosomal protein DnaI
		K05787	HupA	DNA-binding protein HU-alpha
		K03530	hupB	DNA-binding protein HU-beta
		K04764	IhfA, HimA	integration host factor subunit alpha
		K05788	IhfB, HimD	integration host factor subunit beta
		K03111	ssb	single-strand DNA-binding protein
	Terminus site-binding protein	*K10748*	Tus, Tau	DNA replication terminus site-binding protein
	DNA methylation enzyme	*K06223*	Dam	DNA adenine methylase [EC:2.1.1.72]
	Prevention of re-replication factors	*K10763*	Hda	DnaA-homolog protein
		K03645	SeqA	negative modulator of initiation of replication
Chromosome partition	MukBEF complex	*K03632*	MukB	chromosome partition protein MukB
		K03804	MukE	chromosome partition protein MukE
		K03633	MukF	chromosome partition protein MukF
	Condensin-like complex	*K03529*	Smc	chromosome segregation protein
		K05896	ScpA	segregation and condensation protein A
		K06024	ScpB	segregation and condensation protein B
	Divisome proteins	*K03585*	AcrA	membrane fusion protein
		K01448	AmiA,AmiB, AmiC	N-acetylmuramoyl-L-alanine amidase [EC:3.5.1.28]
		K13052	DivIC, DivA	cell division protein DivIC
		K03590	FtsA	cell division protein FtsA
		K05589	FtsB	cell division protein FtsB
		K09812	FtsE	cell division transport system ATP-binding protein
		K03587	FtsI	cell division protein FtsI [EC:2.4.1.129]
		K03466	FtsK, SpoIIIE	DNA segregation ATPase FtsK/SpoIIIE, S-DNA-T family
		K03586	FtsL	cell division protein FtsL
		K03591	FtsN	cell division protein FtsN
		K03589	FtsQ	cell division protein FtsQ
		K03588	FtsW, SpoVE	cell division protein FtsW
		K09811	FtsX	cell division transport system permease protein
		K03531	FtsZ	cell division protein FtsZ
		K09888	ZapA	cell division protein ZapA
		K03528	ZipA	cell division protein ZipA
	Inhibitors of FtsZ assembly	*K04074*	DivIVA	cell division initiation protein
		K06286	EzrA	septation ring formation regulator

		K03610	MinC	septum site-determining protein MinC
		K03609	MinD	septum site-determining protein MinD
		K03608	MinE	cell division topological specificity factor
		K05501	SlmA, Ttk	TetR/AcrR family transcriptional regulator
		K09772	SepF	cell division inhibitor SepF
		K13053	SulA	cell division inhibitor, FtsZ assembly inhibitor
	Other chromosome partitioning proteins	*K04095*	Fic	cell filamentation protein
		K04094	Gid, TrmFO	methylenetetrahydrofolate--tRNA-[uracil-5-)-methyltransferase [EC:2.1.1.74]
		K03495	GidA, MnmG, MTO1	tRNA uridine 5-carboxymethylaminomethyl modification enzyme
		K03501	GidB, RsmG	16S rRNA [guanine527-N7)-methyltransferase [EC:2.1.1.170]
		K03569	MreB	rod shape-determining protein MreB and related proteins
		K03570	MreC	rod shape-determining protein MreC
		K03571	MreD	rod shape-determining protein MreD
		K03593	Mrp	ATP-binding protein involved in chromosome partitioning
		K03496	ParA, Soj	chromosome partitioning protein
		K03497	ParB, Spo0J	chromosome partitioning protein, ParB family
		K02621	ParC	topoisomerase IV subunit A [EC:5.99.1.-]
		K02622	ParE	topoisomerase IV subunit B [EC:5.99.1.-]
		K11686	RacA	chromosome-anchoring protein RacA
		K05837	RodA, MrdB	rod shape determining protein RodA
		K03645	SeqA	negative modulator of initiation of replication
		K03733	XerC	integrase/recombinase XerC
		K04763	XerD	integrase/recombinase XerD
Nucleoid	HNS (histone-like nucleoid structuring protein)	*K03746*	H-NS	DNA-binding protein H-NS
		K11685	StpA	DNA-binding protein StpA
	HU (heat unstable protein)	*K05787*	HupA	DNA-binding protein HU-alpha
		K03530	HupB	DNA-binding protein HU-beta
	IHF (integration host factor)	*K04764*	IhfA, HimA	integration host factor subunit alpha
		K05788	IhfB, HimD	integration host factor subunit beta
	Other nucleoid associated proteins	*K05516*	CbpA	curved DNA-binding protein
		K12961	DiaA	chromosomal replication initiator protein
		K02313	DnaA	DnaA initiator-associating protein
		K04047	Dps	starvation-inducible DNA-binding protein
		K03557	Fis	Fis family transcriptional regulator, factor for inversion stimulation protein
		K03666	Hfq	host factor-I protein
		K05596	IciA	chromosome initiation inhibitor, LysR family transcriptional regulator
		K03719	Lrp	leucine-responsive regulatory protein, Lrp/AsnC family transcriptional regulator
		K05804	Rob	right origin-binding protein, AraC family transcriptional regulator

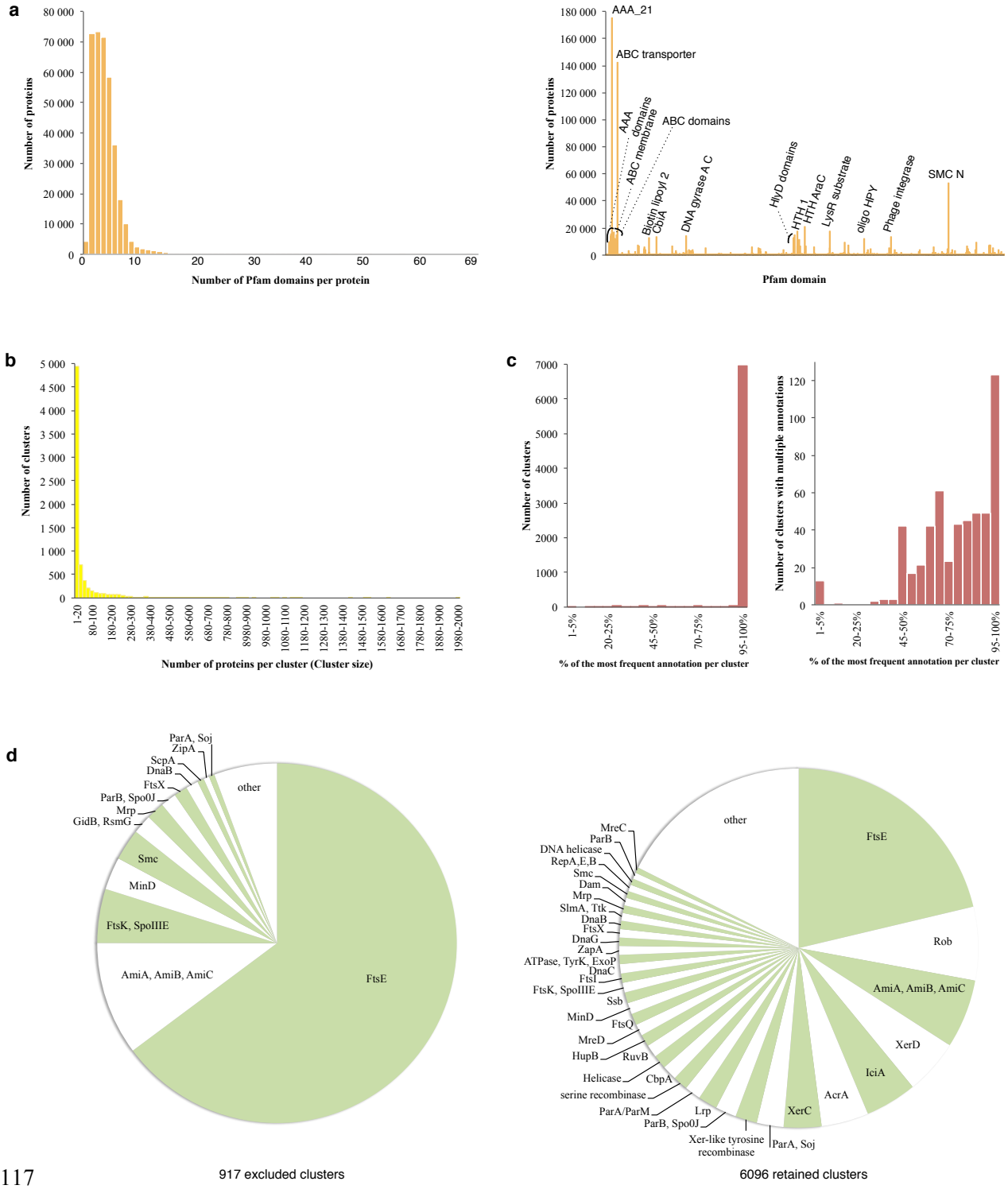

Figure 3. Properties of the IS clustering

(a) Frequency distribution of the 358,624 putative IS protein homologues according to their number of functional domains (0 to 69) per protein (left), and occurrences of the 1711 functional Pfam domains (right). The 20 top most frequently encountered functional domains are indicated. (b) Size distribution of the 7013 clusters, each comprising from a single to 1990 proteins. (c) Percentage distribution of the most frequent annotation per cluster among all clusters (left) and among clusters with multiple annotations (right). (d) Distribution of the most frequent annotation per cluster among the 917 excluded clusters (left) and the 6096 clusters retained for the analysis (right).

We then inferred 7013 homology groups using a clustering procedure and named the clusters after the most frequent annotation found among their proteins (Figure 3b,c). Most clusters were characterized by a single annotation whilst the remaining few (4.7%) each harbored from 2 to 710 annotations, the most frequent annotation in a cluster generally representing more than half of all annotations (Figure 3c). The removal of false positives left 267,497 IS protein homologues distributed in 6096 clusters (Figure 3d) and coded by 4928 replicons out of the initial replicon dataset. Following the Genbank/RefSeq annotations, our final dataset comprised 2016 complete genome sets corresponding to 3592 replicons (2016 chromosomes, 129 SERs, and 1447 plasmids) and 1336 plasmid genomes (Supplementary table 1), irregularly distributed across the bacterial phylogeny (Figure 4a). Multi-ER genomes are observed in 5.0% of all represented bacterial genera and constitute 5.7% of the complete genomes (averaged over genera) available at the time of study (Figure 4b). They are merely incidental (0.2% in Firmicutes) or reach up to almost one third of the genomes (30.1% in β-Proteobacteria) depending on the lineage, and are yet to be observed in most bacterial phyla, possibly because of the poor representation of some lineages. Although found in ten phyla, they occur more than once per genus in only three of them: Bacteroidetes, Proteobacteria and Spirochaetae.

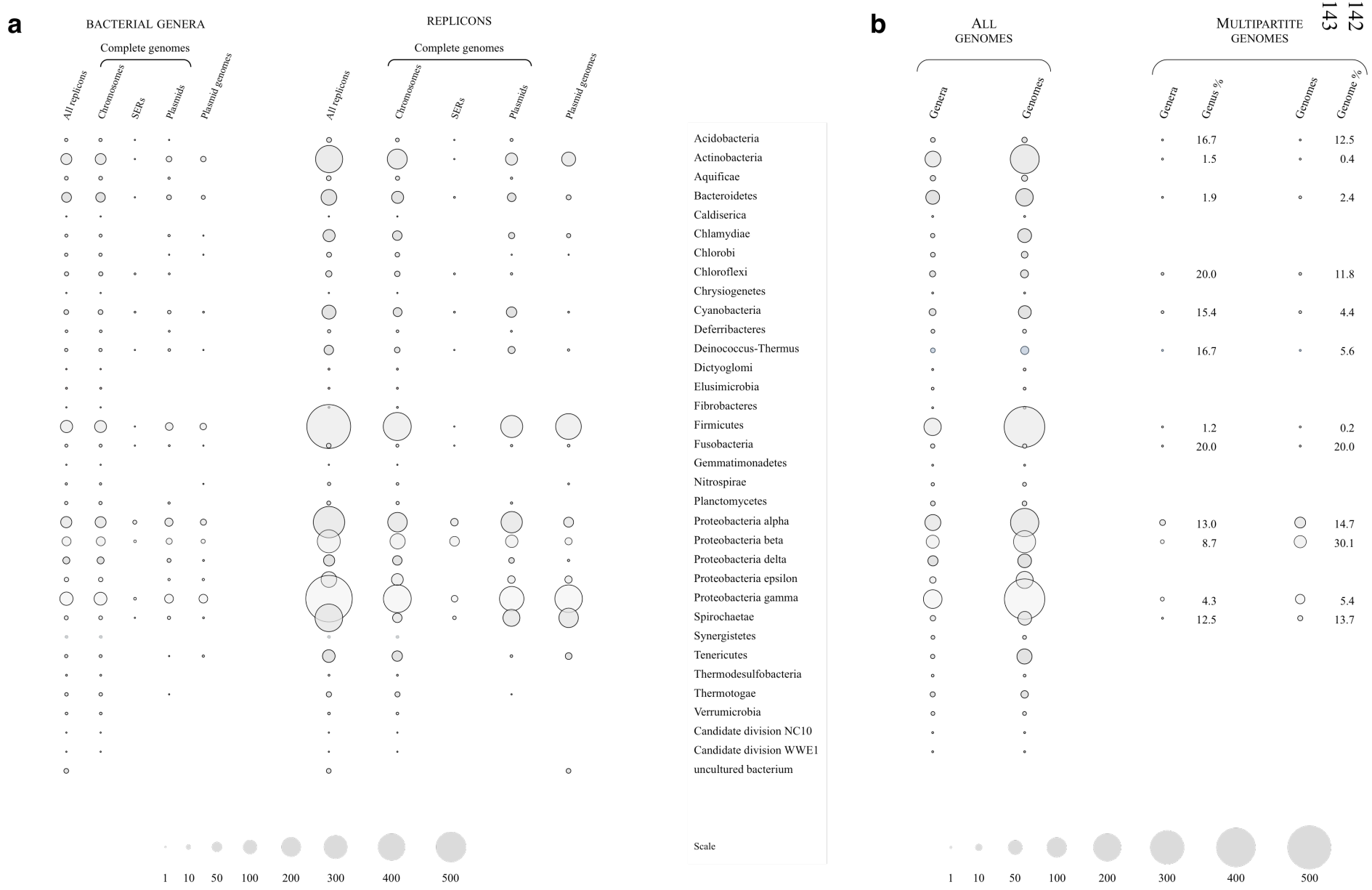

Figure 4. Taxonomic structure of the replicon dataset

Numbers of replicons (a) and complete genomes (b), and represented bacterial genera are shown according to datasets and host taxonomy. Surfaces represent the numbers of bacterial genera, replicons or genomes within each category. Percentages of multipartite genomes and corresponding bacterial genera are calculated for each host phylum or class (Proteobacteria).

Exploration of the replicon diversity

We explored the differences and similarities of the bacterial replicons with regard to their IS usage using a data mining and machine learning approach (Methods). The 6096 retained IS clusters were used as distinct variables to ascribe each of the 4928 replicons with a vector according to its IS usage profile. We transformed these data into bipartite graphs depending on the number of proteins from the IS clusters coded by each replicon. Bipartite graphs display both the vectors (replicons) and the variables (protein clusters) together with their respective connections, and allow the interactive exploration of the data. The majority of the replicons are interconnected (Figure 5) as testimony of the shared evolutionary history of their IS sequences. Chromosomes and plasmids form overall distinct groups and communities with varying degree of connectivity depending on their functional specificities (Figure 5a) as well as on the bacterial taxonomy of their hosts (Figure 5c). They nonetheless share many ISs, bearing witness to the continuity of the genomic material and the extensive exchange of genetic material within bacterial genomes. The occurrence of poorly IS cluster-connected plasmids within a group of chromosomes did not consistently reflect a true relationship and rather resulted from shared connections to a very small number (as low as one) of common ISs. While being interconnected to both chromosomes and plasmids *via* numerous IS clusters, the SERs generally stand apart from either these types of replicons and gather at the chromosome-plasmid interface (Figure 5a,b). Their IS usage is neither chromosome-like nor plasmid-like, suggesting that they may constitute a separate category of replicons. This is most tangible in the case of the proteobacterial lineages where SERs occur most frequently (top of Figure 5b).

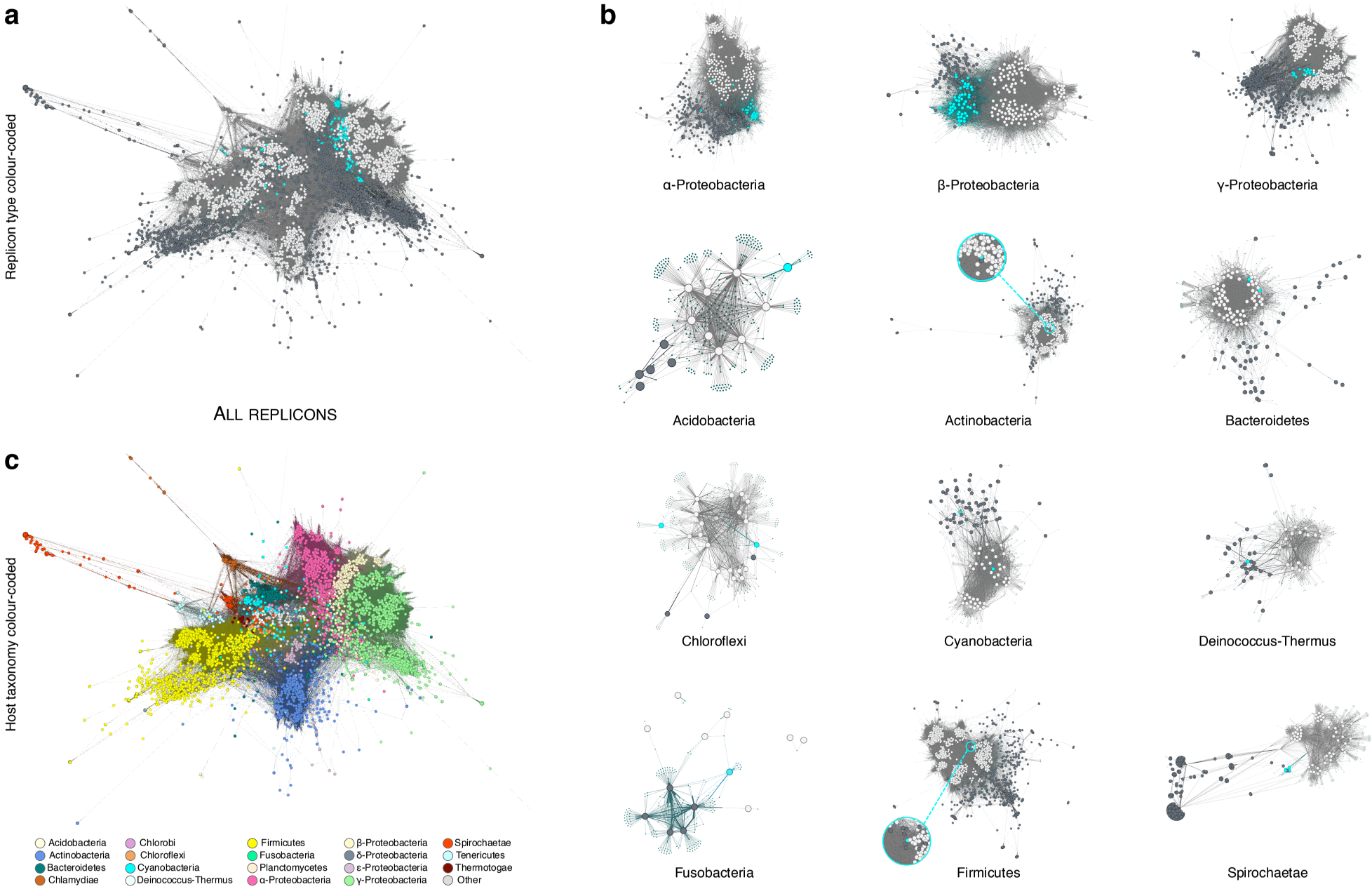

Figure 5. Visualisation of the replicon IS-based relationshipss

Gephi-generated bipartite-graphs for the whole dataset (a and b) or groups of replicons following the host taxonomy (c). Nodes correspond to the replicons (large dots) or the clusters of IS proteins (small dots). Edges linking replicons and protein clusters reflect the presence on a replicon of at least one protein of a protein cluster. Colouring according to replicon type (a and c): chromosomes (white), plasmids (grey), and SERs (blue), or according to host taxonomy (b).

All SERs in the β- and γ-Proteobacteria, and most in the α-Proteobacteria are linked to remarkable chromosome-type IS clusters, such as AcrA, IciA, FtsE, HN-S and Lrp, as well as to plasmid-like ParA/ParB, Rep and PSK IS clusters. A similar pattern is observed for the SERs in actinobacterium *Nocardiopsis dassonvillei,* firmicute *Butyrivibrio proteoclasticus*, and chloroflexi *Sphaerobacter thermophilus* and *Thermobaculum terrenum* (Figure 5b). Interestingly, DNA primase DnaG-annotated clusters connect the SERs present in all but one *Burkholderia* species (β-Proteobacteria) as well as the chromosomes of all other bacteria. Since the sole exception, *B. rhizoxinica*, possesses a SER-less reduced genome as an adaption to intracellular life, the *Burkholderia* SERs likely originated from a single event prior to the diversification of the genus, possibly in relation to the speciation event that gave rise to this lineage. The second SERs harbored by only some *Burkholderia* species exhibit a higher level of interconnection to plasmids, as do the SERs in α-proteobacterium *Sphingobium*, cyanobacterium *Cyanothece* sp. ATCC 51142, *Deinococcus radiodurans* (Deinococcus-Thermus) and fusobacterium *Ilyobacter polytropus*. This points to an incomplete stabilization of the SERs into the genome that may reflect a recent, ongoing, event of integration and/or differing selective pressures at play depending on the bacterial lineages. At odds with these observations, some SERs group unambiguously with chromosomes. The SERs in α-Proteobacteria *Asticcacaulis excentricus* and *Paracoccus denitrificans*, Bacteroidetes *Prevotella intermedia* and *P. melaninogenica*, acidobacterium *Chloracidobacterium thermophilum*, and cyanobacterium *Anabaena* sp. 90 bear higher levels of interconnection to chromosomes than to plasmids or other SERs. Indeed, the SERs in *Prevotella* spp. are hardly linked to plasmids, and the few plasmid-like IS proteins that *C. thermophilum* SER codes (mostly Rep, Helicase and PSK), albeit found in plasmids occurring in other phyla, are observed in none of the

Acidobacteria plasmids. An extreme situation is met in *Leptospira* spp. (Spirochaetae) whose SERs are each linked to only three or four (out of a total of six) chromosome-like IS clusters, always including ParA and ParB. Interestingly, the ParA cluster appears to be specific to Spirochaetae chromosomes with the notable exception of one plasmid found in Leptospiraceae *Turneriella parva*.

IS-based relationships of the replicons

We submitted the bipartite graph of the whole dataset to a community structure detection algorithm (INFOMAP) that performs a random walk along the edges connecting the graph vertices. We expected the replicon communities to be trapped in high-density regions of the graph. We also performed a dimension reduction by Principal Component Analysis followed by a hierarchical clustering procedure (WARD). The clustering solutions (Supplementary tables 2 and 3) were meaningful (high values reached by the stability criterion scores), and biologically relevant (efficient separation of the chromosomes from the plasmids; high *homogeneity* values) using either method (Table 3). In another experiment, we considered each genus as a unique sample and averaged the variables over the replicons of the different species for each replicon type. The aim was to control for the disparity in taxon representation of the replicons. This dataset produced overall similar albeit slightly less stable clusters (lower *homogeneity* values). Taxonomically homogeneous clusters of chromosomes were best retrieved using the coupling of dimension reduction and hierarchical clustering with a large enough number of clusters (*homogeneity* scores up to 0.93). In turn, the community detection algorithm was more efficient in recovering the underlying taxonomy of replicons (higher value of *completeness*), and was sole able to identify small and scattered plasmid clusters (Supplementary tables 2 and 3).

Table 3. Evaluation of the replicon IS-based clusterings

		INDEX[a]	USING IS PROTEIN SEQUENCES				USING IS FUNCTIONS	
	CLUSTERING		INFOMAP		PCA+ WARD[b]		PCA+ WARD[b]	
PROCEDURE	Dataset[c]		V^R	$\bar{V}^R_{genus}$	V^R	$\bar{V}^R_{genus}$	V^R_f	$\bar{V}^R_{f,genus}$
	Parameters		500 iterations		$\begin{cases} k = 200 \\ pc = 30 \end{cases}$	$\begin{cases} k = 200 \\ pc = 30 \end{cases}$	$\begin{cases} k = 50 \\ pc = 4 \end{cases}$	$\begin{cases} k = 20 \\ pc = 4 \end{cases}$
	Number of clusters		223	77	175	75	49	19
	PCA explained variance				57%	58%	87%	85%
	Stability criterion (Δ^{Kl})[d]		0.82	0.76	0.85	0.74	0.80	0.71
EVALUATED SEPARATION	Chromosomes *vs.* Plasmids	*homogeneity*	0.82	0.63	0.93	0.83	0.85	0.68
		completeness	0.15	0.15	0.25	0.20	0.30	0.23
		V-measure	0.25	0.24	0.43	0.32	0.44	0.35
	Chromosomes *per* host phylum	*homogeneity*	0.93	0.69	0.93	0.80	0.50	0.44
		completeness	0.60	0.61	0.35	0.40	0.27	0.33
		V-measure	0.73	0.65	0.51	0.53	0.35	0.38
	Chromosomes *per* host class	*homogeneity*	0.85	0.64	0.93	0.80	0.47	0.37
		completeness	0.80	0.82	0.16	0.58	0.36	0.41
		V-measure	0.82	0.72	0.66	0.67	0.41	0.39
	Plasmids *per* host phylum	*homogeneity*	0.88	0.78	0.06	0.01	0.02	0.02
		completeness	0.33	0.35	0.16	0.14	0.10	0.30
		V-measure	0.48	0.48	0.08	0.02	0.03	0.03
	Plasmids *per* host class	*homogeneity*	0.84	0.74	0.07	0.02	0.03	0.02
		completeness	0.43	0.51	0.28	0.36	0.25	0.28
		V-measure	0.57	0.60	0.12	0.03	0.05	0.03

[a] *V-measure* according to Rosenberg and Hirschberg (2007)

[b] *k*: number of input clusters; *pc*: principal components used in WARD

[c] V^R_f: Ensemble of all IS function-based replicon vectors (v^r_f); $\bar{V}^R_{f,genus}$: Ensemble of IS function-based genus-normalized replicon vectors ($v^r_{f,genus}$)

[d] Stability criterion according to Hennig (2007)

The plasmid clusters obtained using PCA+WARD lacked taxonomical patterning and, although highly stable, only reflected the small Euclidian distances existing among the plasmid replicons (*e.g.*, one cluster of 2656 plasmids had a stability score of 0.975). The

clusters obtained with INFOMAP mirrored the taxonomical structure of the data, suggesting that the taxonomic signal, expected to be associated to the chromosomes, is preserved among the IS protein families functionally specifying the plasmids. The presence of a majority of the SERs amongst the chromosome clusters generated by INFOMAP confirmed the affinities between these two genomic elements and the clear individuation of the SERs from the plasmids. However, the larger number of chromosomal ISs often caused the PCA+WARD approach to place SERs into plasmid clusters. The SERs in *Butyrivibrio*, *Deinococcus*, *Leptospira* and *Rhodobacter* spp. grouped consistently with plasmids while the SERs in *Vibrionaceae* and *Brucellaceae* formed specific clusters (Table 4). Burkholderiales and *Agrobacterium* SERs, whose homogenous clusters tended to be unstable, exhibited a higher affinity to plasmids overall. The SERs of *Asticaccaulis*, *Paracoccus* and *Prevotella* spp. associated stably with chromosomes using the two clustering methods (Table 4a,b) and possess IS profiles that set them apart from both the plasmids and the other SERs.

Table 4. IS protein cluster-based unsupervised classification of SERs

a. INFOMAP clustering solution

Bacterial genus	C [a]	CHR%	SER%	PLD%	$wBHI$ [b]	$\overline{\Delta^C}$ [c]	$\overline{\Delta^r}$ [d]
Agrobacterium	3	38	35	27	0.90	0.47	0.61
Aliivibrio	1	0	100	0	1.00	0.95	1.00
Anabaena	1	98	1	1	1.00	0.90	1.00
Asticcacaulis	1	96	1	3	1.00	0.97	1.00
Brucella	1	0	95	5	1.00	0.87	1.00
Burkholderia	2	64	17	19	0.99	0.77	0.99
Butyrivibrio	1	0	50	50	1.00	0.83	1.00
Chloracidobacterium	1	91	<1	9	0.82	0.86	0.00
Cupriavidus	1	73	18	9	0.99	0.72	1.00
Cyanothece	1	0	6	94	0.89	0.61	0.33
Deinococcus	1	0	4	96	0.71	0.61	1.00
Ilyobacter	1	91	<1	9	0.82	0.86	0.25
Leptospira	1	0	88	12	1.00	1.00	1.00

Nocardiopsis	1	91	<1	9	0.97	0.97	1.00
Ochrobactrum	1	0	95	5	1.00	0.87	*n.a.n.*[e]
Paracoccus	1	96	1	3	1.00	0.97	1.00
Photobacterium	1	96	1	3	0.99	0.79	1.00
Prevotella	1	96	2	2	0.95	0.92	1.00
Pseudoalteromonas	1	96	1	3	0.99	0.79	0.56
Ralstonia	1	73	18	9	0.99	0.72	1.00
Rhodobacter	1	0	40	60	1.00	0.71	1.00
Ensifer (*Sinorhizobium*)	2	0	2	98	0.96	0.65	0.67
Sphaerobacter	1	0	50	50	1.00	1.00	1.00
Sphingobium	2	77	1	22	0.95	0.90	0.50
Thermobaculum	1	91	<1	9	0.82	0.86	1.00
Variovorax	1	73	18	9	0.99	0.72	0.90
Vibrio	1	0	100	0	1.00	0.95	0.89

[a] number of clusters containing SERs of a given bacterial genus
[b] weighted biological homogeneity index value for the phylum of the replicons in the clusters
[c] mean value of the cluster stability estimator, weighted by the cluster sizes
[d] mean value of the SER stability estimator for a given bacterial genus
[e] "*n.a.n.*", standing for "not a number", indicates that the replicon appeared in none of the bootstrap replications performed in the clustering procedure

b. PCA+WARD clustering solution

Bacterial genus	C[a]	CHR%	SER%	PLD%	*wBHI*[b]	$\overline{\Delta^C}$ [c]	$\overline{\Delta^r}$ [d]
Agrobacterium	2	0	29	71	0.94	0.76	1.00
Aliivibrio	2	0	56	44	1.00	0.60	0.33
Anabaena	1	98	2	0	0.97	0.84	0.00
Asticcacaulis	1	88	8	4	1.00	0.88	1.00
Brucella	2	0	33	67	0.96	0.53	0.97
Burkholderia	7	0	79	21	0.97	0.69	0.84
Butyrivibrio	1	<1	1	99	0.27	0.98	1.00
Chloracidobacterium	1	<1	1	99	0.27	0.98	1.00
Cupriavidus	2	0	92	8	1.00	0.69	0.92
Cyanothece	1	<1	1	99	0.27	0.98	1.00
Deinococcus	1	<1	1	99	0.27	0.98	1.00
Ilyobacter	1	<1	1	99	0.27	0.98	1.00
Leptospira	1	<1	1	99	0.27	0.98	1.00
Nocardiopsis	1	0	2	98	0.58	0.40	1.00
Ochrobactrum	1	0	100	0	1.00	1.00	1.00
Paracoccus	1	88	8	4	1.00	0.88	1.00
Photobacterium	1	0	100	0	1.00	0.55	1.00
Prevotella	2	95	5	0	1.00	0.73	0.50
Pseudoalteromonas	2	<1	1	99	0.28	0.82	0.83
Ralstonia	1	0	68	32	1.00	0.81	0.83
Rhodobacter	2	0	6	94	0.65	0.43	0.58
Ensifer (*Sinorhizobium*)	2	0	21	79	0.94	0.46	0.25
Sphaerobacter	1	0	20	80	0.93	0.52	0.50

Sphingobium	1	0	39	61	1.00	0.66	0.83
Thermobaculum	1	<1	1	99	0.27	0.98	1.00
Variovorax	1	0	67	33	1.00	0.48	0.00
Vibrio	2	0	56	44	1.00	0.60	0.79

250 [a] number of clusters containing SERs of a given bacterial genus
251 [b] weighted biological homogeneity index value for the phylum of the replicons in the clusters
252 [c] mean value of the cluster stability estimator, weighted by the cluster sizes
253 [d] mean value of the SER stability estimator for a given bacterial genus

254 We reached similar conclusions when performing a PCA+WARD clustering using the
255 117 functional annotations of the IS protein clusters rather than the IS clusters
256 themselves (Tables 3 and 5; Supplementary table 4).

257 **Table 5. Function-based unsupervised classification of SERs using PCA+WARD**

Bacterial genus	C[a]	CHR%	SER%	PLD%	*wBHI*[b]	$\overline{\Delta^c}$[c]	$\overline{\Delta^r}$[d]
Agrobacterium	3	64	21	15	0.86	0.60	0.81
Aliivibrio	1	0	70	30	1.00	0.70	0.67
Anabaena	1	77	4	19	0.21	0.64	1.00
Asticcacaulis	1	99	1	0	0.51	0.60	1.00
Brucella	1	43	32	25	0.75	0.80	1.00
Burkholderia	6	31	42	27	0.92	0.68	0.81
Butyrivibrio	1	77	4	19	0.21	0.64	1.00
Chloracidobacterium	1	1	<1	99	0.29	0.98	0.00
Cupriavidus	1	5	95	0	1.00	0.66	0.66
Cyanothece	1	1	<1	99	0.29	0.98	1.00
Deinococcus	1	1	<1	99	0.29	0.98	1.00
Ilyobacter	1	77	4	19	0.21	0.64	1.00
Leptospira	1	1	<1	99	0.29	0.98	1.00
Nocardiopsis	1	77	4	19	0.21	0.64	1.00
Ochrobactrum	1	90	8	2	1.00	0.40	0.73
Paracoccus	1	92	5	3	0.89	0.32	0.53
Photobacterium	1	0	70	30	1.00	0.70	0.36
Prevotella	2	86	3	11	0.34	0.62	0.50
Pseudoalteromonas	1	77	4	19	0.21	0.64	0.29
Ralstonia	1	0	70	30	1.00	0.70	0.22
Rhodobacter	2	27	32	41	0.84	0.73	0.83
Ensifer (*Sinorhizobium*)	2	25	48	27	0.86	0.76	0.63
Sphaerobacter	1	100	<1	0	0.35	0.60	1.00
Sphingobium	2	62	17	21	0.34	0.64	0.86
Thermobaculum	1	77	4	19	0.21	0.64	1.00
Variovorax	1	0	70	30	1.00	0.70	1.00

Vibrio	4	31	37	32	0.97	0.57	0.92

[a] number of clusters containing SERs of a given bacterial genus
[b] weighted biological homogeneity index value for the phylum of the replicons in the clusters
[c] mean value of the cluster stability estimator, weighted by the sizes of the clusters
[d] mean value of the SER stability estimator for a given bacterial genus

Remarkably, in this latter analysis, the chromosomes in the multipartite genomes of *Prevotella intermedia* and *P. melaninogenica* were more similar to plasmids than to other groups of chromosomes and to single chromosomes in other *Prevotella* species (*P. denticola* and *P. ruminicola*).

SER-specifying IS functions

Next, we searched which of the IS functions are specific to the SERs. We performed several logistic regression analyses to identify over- or under-represented ISs and to assess their respective relevance to each class of replicons. Because of their comparatively small number, all SERs were assembled into a single group despite their disparity. A hundred and one IS functionalities (96% of KEGG-annotated chromosome-like functions and 72% of ACLAME-annotated plasmid-like functions) were significantly enriched in one replicon category over the other (Table 6). The large majority of the IS functions differentiates the chromosomes from the plasmids. The latter are only determined by ISs corresponding to ACLAME annotations Rep, Rop and TrfA, involved in initiation of plasmid replication, and ParA and ParB, dedicated to plasmid partition. Some KEGG-annotated functions, *e.g.,* DnaA, DnaB or FtsZ, appear to be more highly specific to chromosomes (higher *OR* values) than others such as DnaC, FtsE or H-NS (lower *OR* values). Strikingly, very few functions distinguish significantly the chromosomes from the SERs, by contrast with plasmids.

Table 6. IS usage comparison between replicon categories

Between classes of replicons logistic regressions for each IS function. Model significance: $0 < P\_value < 0.01$: significant; $0.01 < P\_value < 0.05$: poorly significant; $0.05 < P\_value$: non significant (not shown). Odd-ratio (*OR*) favouring the first class: $10^0 \leq OR$, or the second class: $OR < 10^0$. IS functions biased to the same order of magnitude in chromosomes and SERs when compared to plasmids are highlighted (blue).

KEGG entries (chromosome-like)	IS function	Chromosomes *vs.* Plasmids		Chromosomes *vs.* SERs		SERs *vs.* Plasmids	
		P_value	*OR*	*P_value*	*OR*	*P_value*	*OR*
REPLICATION	CbpA	8.20×10^{-27}	2,608.4	9.90×10^{-13}	22.8	5.60×10^{-07}	36.1
	Dam	6.90×10^{-16}	16.7	3.60×10^{-02}	2.0	2.40×10^{-02}	4.3
	DiaA	1.50×10^{-15}	81.9	1.20×10^{-03}	38.4		
	DnaA	3.00×10^{-44}	2,118.9	1.10×10^{-19}	239.6	3.50×10^{-03}	8.3
	DnaB	1.10×10^{-43}	1,992.9	5.10×10^{-19}	429.4	8.20×10^{-03}	3.7
	DnaB2	6.70×10^{-03}	12.6				
	DnaC	6.00×10^{-12}	2.6			4.60×10^{-02}	1.5
	DnaG	2.10×10^{-50}	1,861.5	1.90×10^{-21}	205.3	2.50×10^{-03}	4.5
	DnaI	5.20×10^{-03}	18.0				
	Dps	9.10×10^{-21}	65.3	3.50×10^{-05}	8.4	8.70×10^{-03}	6.7
	Fis	5.80×10^{-07}	180.9	3.30×10^{-03}	7.9	1.40×10^{-02}	25.1
	Hda	7.30×10^{-07}	149.1	5.30×10^{-03}	7.9	1.90×10^{-02}	18.0
	Hfq	1.40×10^{-12}	121.7	3.00×10^{-04}	6.9	8.10×10^{-04}	19.3
	H-NS	1.10×10^{-05}	2.8			3.80×10^{-04}	2.8
	HupA	2.70×10^{-04}	15.1				
	HupB	1.20×10^{-53}	97.6	2.30×10^{-08}	6.7	2.40×10^{-07}	11.6
	IciA	7.10×10^{-20}	3.2			4.50×10^{-07}	1.8
	IhfA, HimA	1.70×10^{-12}	63.8	1.40×10^{-03}	10.5	4.90×10^{-02}	6.9
	IhfB, HimD	1.20×10^{-14}	68.4	4.90×10^{-04}	8.4	8.40×10^{-03}	9.9
	Lrp	1.60×10^{-19}	8.4			5.40×10^{-11}	8.1
	Rob	6.30×10^{-19}	5.3			3.40×10^{-08}	4.2
	SeqA	1.60×10^{-03}	25.9				
	ssb	5.90×10^{-41}	298.3	5.00×10^{-18}	160.6		
PARTITION	Fic	3.10×10^{-09}	10.3			8.60×10^{-03}	7.2
	GidA, MnmG,	5.20×10^{-13}	1,477.2	2.90×10^{-08}	110.6	4.30×10^{-02}	18.2
	GidB, RsmG	6.70×10^{-17}	6,059.9	2.20×10^{-15}	252.5	9.00×10^{-03}	32.2
	MreB	1.30×10^{-21}	1,598.2	3.90×10^{-12}	40.1	1.40×10^{-05}	24.1
	MreC	2.90×10^{-11}	1,311.2	1.30×10^{-08}	46.3	8.90×10^{-03}	32.8
	MreD	1.80×10^{-08}	459.2	6.80×10^{-05}	19.8	1.90×10^{-02}	18.2
	Mrp	6.60×10^{-17}	2,599.3	1.30×10^{-14}	35.0	2.50×10^{-05}	86.2
	MukB	2.30×10^{-03}	27.4			1.90×10^{-02}	18.2
	MukE	3.10×10^{-03}	21.0			1.90×10^{-02}	18.2
	MukF	3.70×10^{-03}	19.6			1.90×10^{-02}	18.2
	ParA, Soj	2.70×10^{-38}	9.9	9.00×10^{-06}	2.6	8.40×10^{-06}	3.8
	ParB, Spo0J	2.50×10^{-44}	13.7	3.00×10^{-03}	2.1	2.30×10^{-06}	4.1
	ParC	3.00×10^{-27}	4,149.3	3.00×10^{-16}	134.0	4.60×10^{-04}	12.3
	ParE	7.30×10^{-26}	5,842.4	5.70×10^{-15}	350.1	2.40×10^{-04}	15.8
	RodA, MrdB	2.80×10^{-12}	1,233.1	9.70×10^{-10}	33.0	2.60×10^{-03}	55.3
	TrmFO, Gid	1.50×10^{-06}	182.5	4.40×10^{-03}	8.3	1.90×10^{-02}	18.0
	XerC	1.70×10^{-43}	55.0	3.10×10^{-08}	8.8	1.80×10^{-04}	6.7
	XerD	1.30×10^{-38}	26.6	4.10×10^{-08}	3.4	2.50×10^{-06}	6.2
SEGREGATION	ScpA	1.40×10^{-11}	789.4	5.70×10^{-07}	42.9	2.10×10^{-02}	16.6
	ScpB	7.50×10^{-32}	102.5	1.80×10^{-07}	25.8		
	SepF	1.80×10^{-07}	68.8	1.40×10^{-02}	12.3		
	SlmA, Ttk	3.80×10^{-09}	52.3	1.20×10^{-02}	4.6	1.50×10^{-02}	7.5
	Smc	1.60×10^{-08}	3,090.5	1.40×10^{-05}	131.9		
	SulA	3.30×10^{-06}	17.5			1.50×10^{-02}	10.7
	AcrA	6.60×10^{-19}	2.8	1.70×10^{-02}	1.1	5.30×10^{-10}	2.7
CELL DIVISION	AmiA, AmiB,	6.40×10^{-36}	46.4	2.90×10^{-10}	8.9	4.60×10^{-03}	3.0
	DivIC, DivA	4.90×10^{-05}	90.5	4.70×10^{-02}	8.1		
	DivIVA	4.10×10^{-06}	128.0	1.10×10^{-02}	13.4		
	EzrA	1.00×10^{-02}	13.7				
	FtsA	9.50×10^{-12}	742.7	2.20×10^{-08}	24.6	2.50×10^{-03}	41.7
	FtsB	1.10×10^{-06}	167.2	5.40×10^{-03}	16.1		
	FtsE	4.20×10^{-24}	2.3	1.30×10^{-06}	1.1	4.00×10^{-11}	1.9
	FtsI	9.80×10^{-09}	47.0	7.00×10^{-16}	3.9	2.20×10^{-07}	76.7
	FtsK, SpoIIIE	2.80×10^{-37}	76.9	2.70×10^{-08}	15.8	1.40×10^{-02}	4.2
	FtsL	1.20×10^{-05}	91.5	2.70×10^{-02}	9.8		
	FtsN	1.60×10^{-04}	53.0				
	FtsQ	1.70×10^{-15}	2,135.0	1.30×10^{-11}	99.3	9.00×10^{-03}	28.8
	FtsW, SpoVE	5.70×10^{-16}	4,266.4	4.40×10^{-16}	87.7	8.20×10^{-04}	55.0
	FtsX	9.30×10^{-12}	972.9	1.30×10^{-08}	13.8	4.80×10^{-04}	146.2
	FtsZ	3.10×10^{-31}	2,747.0	1.20×10^{-19}	101.6	9.70×10^{-04}	16.5
	MinC	4.40×10^{-09}	172.3	1.20×10^{-02}	3.0	5.80×10^{-05}	76.8
	MinD	3.10×10^{-19}	42.8	1.60×10^{-04}	2.3	5.40×10^{-11}	81.5
	MinE	9.00×10^{-09}	152.9	3.10×10^{-02}	2.6	5.90×10^{-05}	75.2
	ZapA	8.20×10^{-09}	602.8	7.40×10^{-06}	17.3	7.30×10^{-03}	56.1
	ZipA	7.90×10^{-05}	66.0				

ACLAME Families (plasmid-like)	CdsD			4.40×10^{-02}	0.1		
REPLICATION	DNA helicase	5.80×10^{-21}	33.6	2.70×10^{-04}	4.1	1.30×10^{-04}	9.8
	Helicase-1	1.60×10^{-27}	71.1	1.90×10^{-13}	20.0	1.10×10^{-04}	4.6
	DNA repair	2.20×10^{-04}	34.0			5.70×10^{-04}	43.6
	primase, LtrC	3.10×10^{-02}	1.8				
	RepA	5.90×10^{-03}	0.7				
	RepAEB	1.70×10^{-16}	0.0	1.90×10^{-04}	0.1		
	RepC					9.60×10^{-03}	2.7
	RepCJE			4.40×10^{-02}	0.1		
	RepRSE	1.30×10^{-02}	0.0	4.90×10^{-02}	0.1		
	RNA polymerase	3.20×10^{-02}	6.3				
	Rop	3.20×10^{-02}	0.0	4.40×10^{-02}	0.1		
	RuvB	1.20×10^{-08}	433.0	5.70×10^{-08}	17.7	1.40×10^{-05}	37.8
	TrfA	1.40×10^{-02}	0.3				
PARTITION	ATPase, TyrK,	2.20×10^{-20}	19.4			8.50×10^{-07}	9.3
	CopG			2.70×10^{-02}	0.2	4.60×10^{-03}	23.1
	DNA-binding protein			4.40×10^{-02}	0.1		
	FtsK, SpoIIIE	1.90×10^{-07}	6.0			9.90×10^{-05}	9.8
	ParA, ParM	1.50×10^{-10}	0.4	4.00×10^{-06}	0.3		
	ParB	5.70×10^{-12}	0.1	1.40×10^{-05}	0.2		
	serine recombinase	2.50×10^{-06}	1.4	1.50×10^{-03}	2.9	1.80×10^{-02}	0.4
	tyrosine recombinase	3.40×10^{-04}	3.3			7.40×10^{-04}	8.7
	Xer-like Tyrosine	7.60×10^{-11}	2.0			6.30×10^{-03}	1.6
MAINTENANCE	Ccd (PSK)	4.60×10^{-02}	3.9				
	HicAB (PSK)	4.30×10^{-05}	25.2			4.80×10^{-03}	15.1
	HigBA (PSK)	3.30×10^{-15}	3.4	2.40×10^{-02}	1.5	1.20×10^{-03}	2.5
	MazEF (PSK)	1.20×10^{-11}	5.2	2.90×10^{-02}	2.6		
	ParC (PSK)			4.40×10^{-02}	0.1		
	ParDE (PSK)	5.50×10^{-08}	2.3			7.80×10^{-05}	3.4
	PhD, Doc (PSK)	3.20×10^{-07}	11.9			2.90×10^{-03}	8.8
	plasmid maintenance			4.40×10^{-02}	0.1		
	RelBE (PSK)	2.70×10^{-08}	3.5			6.10×10^{-04}	4.2
	VapBC/Vag (PSK)	1.20×10^{-09}	3.9			1.40×10^{-05}	5.8

Chromosome-signature ISs are also present on the SERs, and some of them are enriched to the same order of magnitude in both classes but not in plasmids (highlighted in Table 6). Among these latter, helicase loader DnaC participates to the replication initiation of the chromosome (Chodavarapu et al., 2016) whilst Walker-type ATPase ParA/Soj interacts with ParB/Spo0J in the *parABS* chromosomal partinioning system, and is required for proper separation of sister origins and synchronous DNA replication (Murray and Errington, 2008). The other ISs have a regulatory role, either locally or globally. Nucleoid-associated proteins (NAPs; Dillon and Dorman, 2010) contribute to the replication regulation: H-NS (histone-like nucleoid structuring protein), IciA (chromosome initiator inhibitor, LysR family transcriptional regulator), MukBEF (condensin), and Rob/ClpB (right arm of the replication origin binding protein/curved DNA-binding protein B, AraC family transcriptional regulator) influence both the conformation and the functions of chromosomal DNA, replication, recombination and

299 repair. The NAPs also have pleiotropic regulatory roles in global regulation of gene
300 transcription depending on cell growth conditions (H-NS, IciA, Lrp (leucine-responsive
301 regulatory protein, Lrp/AsnC family transcriptional regulator), and Rob/ClpB).
302 Similarly, the membrane fusion protein AcrA is a growth-dependent regulator, mostly
303 known for its role as a peripheral scaffold mediating the interaction between AcrB and
304 TolC in the AcrA-AcrB-TolC Resistance-Nodule-cell Division-type efflux pump that
305 extrudes from the cell compounds that are toxic or have a signaling role (Du et al.,
306 2018). It is central to the regulation of cell homeostasis and proper development (Anes
307 et al., 2015; Du et al., 2018; Webber et al., 2009) as well as biofilm formation (Alav et
308 al., 2018). Fic (cell filamentation protein) targets the DNA gyrase B (GyrB) to regulate
309 the cell division and cell morphology (Lu et al., 2018) whereas SulA inhibits FtsZ
310 assembly, hence causing incomplete cell division and filamentation (Chen et al, 2012).
311 FtsE is involved in the Z-ring assembly and the initiation of constriction, and in late
312 stage cell separation (Meier et al, 2017).

313 The main divergence between SERs and chromosomes lies in the distribution patterns of
314 the ACLAME-annotated ISs ($OR < 10^0$ in the chromosomes *vs.* SERs comparison). Their
315 higher abundance on the SERs suggests a stronger link of SERs to plasmids. This
316 pattern may also arise from the unbalanced taxon representation in our SER dataset due
317 to a single bacterial lineage. For example, the presence of RepC is likely to be specific to
318 Rhizobiales SERs (Pinto et al., 2012).

319 **Identification of candidate SERs**

320 Since the IS profiles constitute replicon-type signatures, we searched for new putative
321 SERs or chromosomes among the extra-chromosomal replicons. We used the IS

functions as features to perform supervised classification analyses with various training sets (Table 7).

Table 7. Performance of the ERT classification procedures

TRAINING SET [a]	CV_{score} [b]	$\sigma_{CV_{score}}$ [c]	OOB_{score} [d]	$\sigma_{OOB_{score}}$ [e]
$\{E_{SER}, E'_{plasmid}\}$	0.96	-	0.96	-
$\{E_{SER}, E'_{plasmid}\}^{it}$	0.92	0.02	0.93	0.02
$\{E_{chromosome}, E'_{plasmid}\}$	1.00	-	1.00	-
$\{E_{SER}, E_{chromosome}\}^{it}$	0.98	0.00	0.98	0.01

[a] $E_{chromosome}$ and E_{SER} are host genus-normalized sets of chromosomes or SERs, respectively (*cf.* Table 13). $E'_{plasmid}$ is derived from the INFOMAP clustering solution, by discarding plasmids belonging to clusters also harbouring SERs or chromosomes, and normalized according to host genus. "*it*" designates the iterative procedure.
[b] Cross-validation score or mean of iteration cross-validation scores.
[c] Standard deviation of iteration cross-validation scores.
[d] Out-of bag estimate or mean of iteration Out-of bag estimates.
[e] Standard deviation of iteration Out-of bag estimates.

The coherence of the SER class (overall high values of the probability for a SER to be assigned to its own class in Tables 7 and 8) confirmed that the ISs are robust genomic markers for replicon characterization. The low SER probability scores presented by a few SERs (Table 8) likely result from a low number of carried ISs (*e.g., Leptospira*), or from the absence in the data of lineage-specific ISs (*e.g.*, SER idiosyncratic replication initiator RtcB of Vibrionaceae).

Table 8. SER probability to belong to the *SER* class

Genus	$\bar{P}_{SER}(SER)$[a]
Agrobacterium	0.90
Aliivibrio	0.87
Anabaena	0.94
Asticcacaulis	0.95

Brucella	0.92
Burkholderia	0.89
Butyrivibrio	0.83
Chloracidobacterium	0.88
Cupriavidus	0.94
Cyanothece	0.86
Deinococcus	0.78
Ensifer/Sinorhizobium	0.90
Ilyobacter	0.88
Leptospira	0.54
Nocardiopsis	0.90
Ochrobactrum	0.96
Paracoccus	0.96
Photobacterium	0.95
Prevotella	0.92
Pseudoalteromonas	0.91
Ralstonia	0.95
Rhodobacter	0.69
Sphaerobacter	0.88
Sphingobium	0.73
Thermobaculum	0.78
Variovorax	0.83
Vibrio	0.76

[a] SER probability, averaged per host genus, to belong to the *SER* class in the supervised classification using $\{E_{SER}, E_{plasmid}\}^{it}$ as training set.

We detected a number of candidate SERs among the plasmids (Table 9a), most of which are essential to the cell functioning and/or the fitness of the organism (*cf.* Box 1). Whereas most belong to bacterial lineages known to harbour multipartite genomes, novel taxa emerge as putative hosts to complex genomes (Rhodospirillales and, to a lesser extent, Actinomycetales). In contrast, our analyses confirmed only one putative SER (*Ruegeria* sp. TM1040) within the *Roseobacter* clade (Petersen et al., 2013). Remarkably, we identified eight candidate chromosomes corresponding to two plasmids, also identified as candidate SERs, that encode ISs hardly found in extra-chromosomal

elements (*e.g.*, DnaG, DnaB, ParC and ParE), and six SERs that part of, or all, our analyses associate to standard chromosomes (Table 9b). Notably, *Prevotella intermedia* SER (CP003503) shows a very high probability (> 0.98) to be a chromosome while its annotated chromosome (CP003502), unique of its kind, falls within the plasmid class. This approach can thus be extended to test the type of replicon for (re)annotation purposes.

Table 9. Identification of ERs among the extra-chromosomal replicons

a. Candidate-SERs identified among plasmids

REPLICON	PROBABILITY[a]
Acaryochloris marina MBIC11017 plasmid pREB1 [CYANOBACTERIA : Chroococcales] (CP000838)	0.578
Acaryochloris marina MBIC11017 plasmid pREB2 [CYANOBACTERIA : Chroococcales] (CP000839)	0.582
Agrobacterium sp. H13-3 plasmid pAspH13-3a [α-PROTEOBACTERIA : Rhizobiales] (CP0022)	0.565
Arthrobacter chlorophenolicus A6 plasmid pACHL01 [ACTINOBACTERIA : Actinomycetales] (CP001342)	0.648
Azospirillum brasilense Sp245 plasmid AZOBR_p1 [α-PROTEOBACTERIA : Rhodospirillales] (HE577328)	0.878
Azospirillum brasilense Sp245 plasmid AZOBR_p2 [α-PROTEOBACTERIA : Rhodospirillales] (HE577329)	0.591
Azospirillum brasilense Sp245 plasmid AZOBR_p3 [α-PROTEOBACTERIA : Rhodospirillales] (HE577330)	0.603
Azospirillum lipoferum 4B plasmid AZO_p1e [α-PROTEOBACTERIA : Rhodospirillales] (FQ311869)	0.722
Azospirillum lipoferum 4B plasmid AZO_p2 [α-PROTEOBACTERIA : Rhodospirillales] (FQ311870)	0.609
Azospirillum lipoferum 4B plasmid AZO_p4 [α-PROTEOBACTERIA : Rhodospirillales] (FQ311872)	0.645
Azospirillum sp. B510 plasmid pAB510a [α-PROTEOBACTERIA : Rhodospirillales] (AP010947)	0.732
Azospirillum sp. B510 plasmid pAB510c [α-PROTEOBACTERIA : Rhodospirillales] (AP010949)	0.545
Azospirillum sp. B510 plasmid pAB510d [α-PROTEOBACTERIA : Rhodospirillales] (AP010950)	0.530
Burkholderia phenoliruptrix BR3459a plasmid pSYMBR3459 [β-PROTEOBACTERIA : Burkholderiales] (CP003865)	0.663
Burkholderia phymatum STM815 plasmid pBPHY01 [β-PROTEOBACTERIA : Burkholderiales] (CP001045)	0.733
Burkholderia sp. YI23 plasmid byi_1p [β-PROTEOBACTERIA : Burkholderiales] (CP003090)	0.846
Clostridium botulinum A3 str. Loch Maree plasmid pCLK [FIRMICUTES : Clostridiales] (CP000963)	0.531
Clostridium botulinum Ba4 str. 657 plasmid pCLJ [FIRMICUTES : Clostridiales] (CP001081)	0.531
Cupriavidus metallidurans CH34 megaplasmid [β-PROTEOBACTERIA : Burkholderiales] (CP000353)	0.883
Cupriavidus necator N-1 plasmid BB1p [β-PROTEOBACTERIA : Burkholderiales] (CP002879)	0.500
Cupriavidus pinatubonensis JMP134 megaplasmid [β-PROTEOBACTERIA : Burkholderiales] (CP000092)	0.513
Deinococcus geothermalis DSM 11300 plasmid1 [DEINOCOCCUS-THERMUS : Deinococcales] (CP000358)	0.622
Deinococcus gobiensis I-0 plasmid P1 [DEINOCOCCUS-THERMUS : Deinococcales] (CP002192)	0.812
Ensifer/Sinorhizobium fredii HH103 plasmid pSfHH103e [α-PROTEOBACTERIA : Rhizobiales] (HE616899)	0.915
Ensifer/Sinorhizobium fredii NGR234 plasmid pNGR234b [α-PROTEOBACTERIA : Rhizobiales] (CP000874)	0.894
Ensifer/Sinorhizobium medicae WSM419 plasmid pSMED01 [α-PROTEOBACTERIA : Rhizobiales] (CP000739)	0.942
Ensifer/Sinorhizobium medicae WSM419 plasmid pSMED02 [α-PROTEOBACTERIA : Rhizobiales] (CP000740)	0.836
Ensifer/Sinorhizobium meliloti 1021 plasmid pSymA [α-PROTEOBACTERIA : Rhizobiales] (AE006469)	0.818
Ensifer/Sinorhizobium meliloti 1021 plasmid pSymB [α-PROTEOBACTERIA : Rhizobiales] (AL591985)	0.949
Ensifer/Sinorhizobium meliloti BL2C plasmid pSINMEB01 [α-PROTEOBACTERIA : Rhizobiales] (CP002741)	0.800
Ensifer/Sinorhizobium meliloti BL2C plasmid pSINMEB02 [α-PROTEOBACTERIA : Rhizobiales] (CP002742)	0.961
Ensifer/Sinorhizobium meliloti Rm41 plasmid pSYMA [α-PROTEOBACTERIA : Rhizobiales] (HE995407)	0.922
Ensifer/Sinorhizobium meliloti Rm41 plasmid pSYMB [α-PROTEOBACTERIA : Rhizobiales] (HE995408)	0.960
Ensifer/Sinorhizobium meliloti SM11 plasmid pSmeSM11c [α-PROTEOBACTERIA : Rhizobiales] (CP001831)	0.877
Ensifer/Sinorhizobium meliloti SM11 plasmid pSmeSM11d [α-PROTEOBACTERIA : Rhizobiales] (CP001832)	0.947
Methylobacterium extorquens AM1 megaplasmid [α-PROTEOBACTERIA : Rhizobiales] (CP001511)	0.538
Novosphingobium sp. PP1Y plasmid Mpl [α-PROTEOBACTERIA : Sphingomonadales] (FR856861)	0.523
Pantoea sp. At-9b plasmid pPAT9B01 [γ-PROTEOBACTERIA : Enterobacteriales] (CP002434)	0.527

Paracoccus denitrificans PD1222 plasmid1 [α-PROTEOBACTERIA : Rhodobacterales] (CP000491)	0.769
Ralstonia solanacearum GMI0 plasmid pGMI0MP [β-PROTEOBACTERIA : Burkholderiales] (AL646053)	0.861
Ralstonia solanacearum Po82 megaplasmid [β-PROTEOBACTERIA : Burkholderiales] (CP002820)	0.865
Ralstonia solanacearum PSI07 megaplasmid [β-PROTEOBACTERIA : Burkholderiales] (FP885891)	0.827
Rhizobium etli CFN 42 plasmid p42e [α-PROTEOBACTERIA : Rhizobiales] (CP000137)	0.700
Rhizobium etli CFN 42 plasmid p42f [α-PROTEOBACTERIA : Rhizobiales] (CP000138)	0.555
Rhizobium etli CIAT 652 plasmid pA [α-PROTEOBACTERIA : Rhizobiales] (CP0010)	0.701
Rhizobium etli CIAT 652 plasmid pC [α-PROTEOBACTERIA : Rhizobiales] (CP001077)	0.792
Rhizobium leguminosarum bv. trifolii WSM1325 plasmid pR132501 [α-PROTEOBACTERIA : Rhizobiales] (CP001623)	0.711
Rhizobium leguminosarum bv. trifolii WSM1325 plasmid pR132502 [α-PROTEOBACTERIA : Rhizobiales] (CP001624)	0.741
Rhizobium leguminosarum bv. *trifolii* WSM2304 plasmid pRLG201 [α-PROTEOBACTERIA : Rhizobiales] (CP001192)	0.777
Rhizobium leguminosarum bv. *trifolii* WSM2304 plasmid pRLG202 [α-PROTEOBACTERIA : Rhizobiales] (CP001193)	0.630
Rhizobium leguminosarum bv. *viciae* 3841 plasmid pRL11 [α-PROTEOBACTERIA : Rhizobiales] (AM236085)	0.731
Rhizobium leguminosarum bv. *viciae* 3841 plasmid pRL12 [α-PROTEOBACTERIA : Rhizobiales] (AM236086)	0.718
Ruegeria sp. TM1040 megaplasmid [α-PROTEOBACTERIA : Rhodobacterales] (CP000376)	0.667
Streptomyces cattleya NRRL 8057 plasmid pSCA [ACTINOBACTERIA : Actinomycetales] (FQ859184)	0.727
Streptomyces cattleya NRRL 8057 plasmid pSCATT [ACTINOBACTERIA : Actinomycetales] (CP003229)	0.702
Streptomyces clavuligerus ATCC 27064 plasmid pSCL4 [ACTINOBACTERIA : Actinomycetales] (CM000914)	0.642
Streptomyces clavuligerus ATCC 27064 plasmid pSCL4 [ACTINOBACTERIA : Actinomycetales] (CM001019)	0.642
Thermus thermophilus HB8 plasmid pTT27 [DEINOCOCCUS-THERMUS : Thermales] (AP008227)	0.500
Thermus thermophilus JL-18 plasmid pTTJL1801 [DEINOCOCCUS-THERMUS : Thermales] (CP0033)	0.557
Tistrella mobilis KA081020-065 plasmid pTM2 [α-PROTEOBACTERIA : Rhodospirillales] (CP003238)	0.578
Tistrella mobilis KA081020-065 plasmid pTM3 [α-PROTEOBACTERIA : Rhodospirillales] (CP003239)	0.797

b. Candidate chromosomes identified among extra-chromosomal replicons

REPLICON	PROBABILITY [a]
Anaeba sp. 90 chromosome chANA02 [CYANOBACTERIA : Chroococcales] (CP003285)	0.638
Asticcacaulis excentricus CB 48 chromosome 2 [α-PROTEOBACTERIA : Caulobacterales] (CP002396)	0.637
Azospirillum brasilense Sp245 plasmid AZOBR_p1 [α-PROTEOBACTERIA : Rhodospirillales] (HE577328)	0.774
Methylobacterium extorquens AM1 megaplasmid [α-PROTEOBACTERIA : Rhizobiales] (CP001511)	0.669
Nocardioides dassonvillei DSM 43111 chromosome 2 [ACTINOBACTERIA : Actinomycetales] (CP002041)	0.539
Paracoccus denitrificans PD1222 chromosome2 [α-PROTEOBACTERIA : Rhodobacterales] (CP000490)	0.778
Prevotella intermedia 17 chromosome II [BACTEROIDETES : Bacteroidales] (CP0033)	0.984
Prevotella melaninogenica ATCC 845 chromosome II [BACTEROIDETES : Bacteroidales] (CP002123)	0.698

[a] Probability for an extra-chromosomal replicon, *i.e.*, plasmid or SER, to belong to the SER (a) or Chromosome (b) class according to the supervised classification procedures.

BOX 1. CHARACTERISTICS OF CANDIDATE SERS

According to the literature, most candidate SERs that we detected among plasmids (Table 9a) were expected to be essential to the cell functioning and/or to the fitness of the organism.

• *Azospirillum* genomes are constituted of multiple replicons, at least one of which is expected to be essential. The largest extra-chromosomal replicon in *A. brasilense* was proposed to be essential for bacterial life (Wisniewski-Dyé et al*.,* 2011) since it encodes well-conserved housekeeping genes involved in DNA replication, RNA metabolism and biosynthesis of nucleotides and cofactors, as well as in transport and protein post-translational modifications. This replicon is unambiguously identified as a SER by our analyses, as are additional replicons found in *A. lipoferum* and *A.* sp. B510, expected homologues

to *A. brasilense* SER (Acosta-Cruz et al*.,* 2012). In contrast, other extra-chromosomal replicons classified as chromids by Wisniewski-Dyé et al*.* (2012) are unlikely to be true essential replicons. They were not retrieved among our candidate SERs.

• In *Rhizobium etli* CFN42, functional interactions among sequences scattered in the different extrachromosomal replicons are required for successful completion of life in symbiotic association with plant roots or saprophytic growth (Brom et al., 2000). p42e (CP000137) is the only replicon other than the chromosome that contains genes involved in the primary metabolism (Landeta et al., 2011; Villaseñor *et al.* 2011) and evades its elimination by co-integration with other replicons including the chromosome (Landeta et al., 2011). Furthermore, homologues to this replicon were identified in the genomes of other *R. etli* strains as well as other *Rhizobium* species: *R. etli* CIAT652 pA, *R. leguminosarum* bv. *viciae* 3841 pRL11, *R. leguminosarum* bv. *trifolii* WSM2304 pRLG202 and *R. leguminosarum* bv. *trifolii* WSM1325 pR132502 (CP001075, AM236085, CP001193, and CP001624, respectively) (Landeta et al., 2011; Villaseñor et al., 2011). These replicons were thus proposed to be secondary chromosomes (Landeta et al., 2011).

• The genome of *Ensifer*/*Sinorhizobium meliloti* AK83 was the single multipartite-annotated *Ensifer*/*Sinorhizobium* genomes present in our dataset. This bacterium carries two large extra-chromosomal replicons that are involved in the establishment of the nitrogen fixation symbiosis with legume plants. pSymA contains most of the genes involved in the nodulation and nitrogen fixation whereas pSymB carries exopolysaccharide biosynthetic genes, also required for the establishment of the symbiosis. Our analyses identifies candidate SERs similar to *S. meliloti* AK83 pSymA and pSymB in other *S. meliloti* strains as well as in *S. fredii* and *S. medicae.* pSymB has been referred to as second chromosome for carrying genes encoding essential house-keeping functions (Blanca-Ordóñez et al., 2010 ; Galardini et al., 2011). It shows a higher level of conservation across strains and species than pSymA (Galardini et al., 2013). pSymA, generally thought to be as stable as pSymB, greatly contribute to the bacterial fitness in the rhizosphere (Blanca-Ordóñez et al., 2010; Galardini et al., 2013).

• The identification of *Methylobacterium extorquens* AM1 1.2 Mb megaplasmid as a SER is supported by its presence in the genome in a predicted one copy number, by its coding a truncated *luxI* gene essential for the operation of two chromosomally-located *luxI* genes, as well as the single *umuDC* cluster involved in SOS DNA repair, and by the presence of a 130 kb region syntenic to a region of similar length in the

chromosome of *Methylobacterium extorquens* strain DM4 (Vuilleumier et al., 2009).

• The megaplasmid (821 kb) in *Ruegeria* sp. TM1040 carries more rRNA operons (3) than the chromosome (1) and several unique genes (Moran et al., 2007). *Ruegeria* sp. TM1040 is the only species in the *Roseobacter* group that possesses a SER. None of the plasmids in the other species included in our datasets qualified as SERs according to our results in contrast to the commonly held view (Petersen et al., 2013).

• In *Burkholderia* genus, additional ERs possess a centromere whose sequence is distinct from, but strongly resembles that of the chromosome centromere (Dubarry et al., 2009). However, these centromeres have a common origin and a plasmid ancestry (Passot et al., 2012). The evolution of these replicons into SERs is best accounted for by the high level of plasticity observed in the *Burkholderia* genomes, with extra-chromosomal replicons going through extensive exchange of genetic material among them as well as with the chromosomes (Maida et al., 2014).

• *Acaryochloris marina* MBIC11017 pREB1 (CP000838) and pREB2 (CP000839) plasmids were identified as candidate SERs. Both these megaplasmids code for metabolic key-proteins, and are thus likely to contribute to the bacterium fitness (Swingley et al., 2008).

• The genomes of *Streptomyces cattleya* NRRL8057 and *S. clavuligerus* ATCC27064 harbour a linear megaplasmid (1.8 Mb) that shows a high probability ($P \approx 0.7$) to be a SER. The megaplasmid of *S. cattleya* NRRL8057 encodes genes involved in the synthesis of various antibiotics and secondary metabolites and is expected to be important to the life of the bacterium in its usual habitat (Barbe et al., 2011; O'Rourke et al., 2009). In *S. clavuligerus* ATCC27064, none of the megaplasmid-encoded genes are expected to belong to the core genome (Medema et al., 2010). However, the megaplasmid is likely to contribute to the bacterium firness. It represents more than 20% of the coding genome and constitutes a large reservoir of genes involved in bioactive compound production and cross-regulation with the chromosome (Medema et al., 2010). Furthermore, *S. clavuligerus* chromosome requires the SER-encoded *tap* gene involved in the telomere replication.

• *Butyrivibrio proteoclasticus* B316 harbours two plasmid, one of which, pCY186 plasmid (CP001813), was identified as a candidate SERs by our analysis, albeit with a low probability (0.56). In support to this, it carries numerous genes coding for proteins involved in replication of the chromosome (Yeoman et al., 2011). The second plasmid in that strain, pCY360 (CP001812), also proposed to be an essential replicon

in that bacterium (Yeoman et al., 2011), presents too low a probability (P = 0.32) in our analysis to qualify as a SER.

DISCUSSION

The SERs clearly stand apart from plasmids, including those that occur consistently in a bacterial species, *e.g.*, *Lactobacillus salivarius* pMP118-like plasmids (Li et al., 2007). The replicon size proposed as a primary classification criterion to separate the SERs from the plasmids (diCenzo and Finan, 2017; Harrison et al., 2010) proves to be inoperative. The IS profiles accurately identify the SERs of *Leptospira* and *Butyrivibrio* despite their plasmid-like size, and unambiguously ascribe the chromosomes in the reduced genomes of endosymbionts (sizes down to 139 kb) to the chromosome class. Conversely, they assign *Rhodococcus jostii* RHA1 1.12 Mb-long pRHL1 replicon to the plasmid class, and do not discriminate the megaplasmids (>350 kb (diCenzo and Finan, 2017)) from smaller plasmids. Plasmids may be stabilized in a bacterial population by rapid compensatory adaptation that alleviates the fitness cost incurred by their presence in the cell (San Millan et al., 2014; Hall et al., 2017; Stalder et al., 2017). This phenomenon involves mutations either on the chromosome only, on the plasmid only, or both, and does not preclude the segregational loss of the plasmid. On the contrary, SERs code for chromosome-type IS proteins that integrate them constitutively in the species genome and the cell cycle. The SERs thence qualify as essential replicons regardless of their size and of the phenotypical/ecological, possibly essential, functions that they encode and which vary across host taxa.

Yet, SERs also carry plasmid-like ISs, suggesting a role for plasmids in their formation. The prevailing opinion assumes that SERs derive from the amelioration of megaplasmids (diCenzo and Finan, 2017; diCenzo et al., 2013; Harrison et al., 2010;

452 MacLellan et al., 2004; Slater et al., 2009): a plasmid bringing novel functions for the
453 adaptation of its host to a new environment is stabilized into the bacterial species
454 genome through the transfer from the chromosome of essential genes (diCenzo and
455 Finan, 2017; Slater et al., 2009). However, the generalized presence of chromosome-like
456 ISs in the SERs of the various taxa with multipartite genomes is unlikely to derive from
457 the action of environment-specific and lineage-specific selective forces. In reverse, all
458 bacteria with similar lifestyle and exhibiting some phylogenetic relatedness may not
459 harbor multiple ERs (*e.g.*, α-proteobacterial nitrogen-fixing legume symbionts). Also,
460 the gene shuttling from chromosome to plasmid proposition fails to account for the
461 situation met in the multipartite genomes of *Asticaccaulis excentricus, Paracoccus*
462 *denitrificans* and *Prevotella* species. Their chromosome-type ISs are evenly distributed
463 between the chromosome and the SER whereas their homologues in the mono- or
464 multipartite genomes of most closely related species are primarily chromosome-coded
465 (see Table 10 for an example). This pattern, mirrored in their whole gene content (Naito
466 et al., 2016; Poirion, 2014), hints at the stemming of the two essential replicons from a
467 single chromosome by either a splitting event or a duplication followed by massive gene
468 loss. Neither mechanism informs on the presence of plasmid-type maintenance
469 machinery on one of the replicons. The severing of a chromosome generates a single
470 true replicon carrying the chromosome replication origin and an origin-less remnant,
471 whilst the duplication of the chromosome produces two chromosomal replicons with
472 identical maintenance systems. Whereas multiple copies of the chromosome are known
473 to cohabit constitutively in polyploid bacteria (Ohtani et al., 2010), the co-occurrence of
474 dissimilar chromosomes bearing identical replication initiation and partition systems is
475 yet to be described in bacteria.

Table 10. IS profiles of *Paracoccus denitrificans vs. Rhodobacter sphaeroides* (Rhodobacterales)

Chromosome-like IS functions coded only by the SER in *P. denitrificans* or *R. sphaeroides* whilst by the chromosome in other Rhodobacterales are indicated by an asterisk. Numbers corresponds to the number of homologues (*P. denitrificans* PD1222) or the pourcentage of function-coding replicons (*R. sphaeroides* and Rhodobacterales genomes).

			Paracoccus denitrificans PD1222			*Rhodobacter sphaeroides*			Other Rhodobacterales		
		IS FUNCTION GROUP	chromosome1 (CP000489)	chromosome2 (CP000490)	plasmid1 (CP000491)	chromosome % (n=12)	SER % (n=12)	plasmid % (n=14)	chromosome % (n=12)	plasmid % (n=33)	
KEGG entry (chromosome-like)	REPLICATION	CbpA		1			100			75	
		Dam		1			50	75		25	
		DnaA	*		1		100			92	
		DnaB	*		1		100			100	
		DnaC					25				3
		DnaG	*		1		100			100	
		Dps		1						50	15
		Fis	*		1		100			75	
		Hda								42	
		Hfq	*		1		100			100	
		H-NS		2	2		100		29	67	9
		HupA								17	
		HupB		1			100			100	
		IciA		1					36	67	
		IhfA, HimA		1			100			100	
		IhfB, HimD	*		1	*		100		100	
		Lrp		4	1	3	100	25	50	100	9
		Rob					25			8	
		ssb		1	3		100	100		100	3
	PARTITION	Fic							7	8	6
		GidA, MnmG, MTO1		1			100			100	
		GidB, RsmG		1			100			100	
		MreB	*		1		100			92	
		MreC	*		1		100			92	
		MreD	*		1		100			92	
		Mrp		1			100			100	
		ParA, Soj		4	1		100			100	9
		ParB, Spo0J		3	1	1	100	75		100	42
		ParC		1	1		100			100	
		ParE		1			100			100	
		RodA, MrdB	*		1		100			92	
		TrmFO, Gid	*		1		100			100	
		XerC		1			100			100	
		XerD		1			100	25	7	100	6
	SEGREGATION	ScpA		1			100			100	
		ScpB		1			100			100	
		Smc		1			100			100	
	CELL DIVISION	AcrA		2	2	*		100	7	58	
		AmiA, AmiB, AmiC		1			100			100	
		FtsA	*		1		100			83	
		FtsE		1			100		7	92	
		FtsI		1			100			92	
		FtsK, SpoIIIE		1			100			100	
		FtsQ	*		1		100			92	
		FtsW, SpoVE			1		100			100	
		FtsX		1			100		7	92	
		FtsZ	*		1		100			100	
		MinC				1					
		MinD				1	75			75	
		MinE				1					
		ZapA		1			100			100	
ACLAME family (plasmid-like)	REPLICATION	DNA helicase					25	50	7	25	
		Helicase-1		1	1		100	50		92	3
		Helicase-2								8	3
		DNA repair								8	
		RepA		2	2				43		42
		RepAEB				1		100	7		15
		RepC		1			50		43	8	24
		RuvB		1			100		7	92	
	PARTITION	ATPase, TyrK, ExoP		2			100	50	14	75	15
		ParA, ParM			1	1		100	100	8	88
		ParB					75	100	93	25	64
		plasmid dimer resolution							14		15
		Serine recombinase		3			25		50	50	30
		Tyrosine recombinase					25		7	33	6
		Xer-like tyrosine recombinase			1		25	50		33	6
		XerD					25				
	MAINTENANCE	Ccd (PSK)							7		
		HicAB (PSK)							7		
		HigBA (PSK)		2					14	17	6
		MazEF (PSK)							7		6
		ParDE (PSK)		2	6		25	50	7	8	15
		PhD, Doc (PSK)							7		
		RelBE (PSK)		1							3
		VapBC/Vag (PSK)		3	2				14	8	9

We propose that the requirement for maintenance system compatibility between co-occurring replicons is the driving force behind the presence of plasmid-type replication initiation and maintenance systems in bacterial SERs. Indeed, genes encoding chromosome-like replication initiators (DnaA) are hardly found on SERs. When they are, in *Paracoccus denitrificans*, *Prevotella intermedia* and *P. melaninogenica*, the annotated chromosome in the corresponding genome does not carry one. Similarly, chromosomal centromeres (*parS*) are found on a single replicon within a multipartite genome, which is the chromosome in all genomes but one. In *P. intermedia* (GCA_000261025.1), both replication initiation and partition systems define the SER as the *bona fide* chromosome and the annotated chromosome as an extra-chromosomal replicon. The harmonious coexistence of different replicons in a cell requires that they use divergent enough maintenance systems. In the advent of a chromosome fission or duplication, the involvement of an autonomously self-replicating element different from the chromosome is mandatory to provide one of the generated DNA molecules with a (non-chromosomal) maintenance machinery.

'Plasmid-first' and 'chromosome-first' hypotheses can be reconciled into a unified, general Fusion-Shuffling-Scission model of SER emergence where a chromosome and a plasmid combine into a cointegrate (Fig. 6). Plasmids are known to merge or to integrate chromosomes in both experimental settings (Brom et al., 2000 ; Guo et al., 2003; Iordănescu, 1975 ; Sýkora, 1992) and the natural environment (Cervantes et al., 2011; Naito et al., 2016; Sýkora, 1992), as are the SER and chromosome of a multipartite genome (Val et al., 2014; Xie et al., 2017; Yamamoto et al., 2018). When integrated, the plasmids/SERs can thus replicate with the chromosome and persist in the bacterial lineage through several generations (Cervantes et al., 2011; Val et al., 2014; Xie et al., 2017). The co-integrate may resolve into its original components (Guo et al., 2003; Val

et al., 2014) or give rise to novel genomic architectures (Guo et al., 2003; Cervantes et al., 2011; Val et al., 2014). The co-integration state likely facilitates inter-replicon gene exchanges and genome rearrangements that may lead to the translocation of large chromosome fragments to the resolved plasmid (Guo et al., 2003; Val et al., 2014). Multiple cell divisions, and possibly several merging-resolution rounds, could provide time and opportunity for the plasmid-chromosome re-assortment to take place, and for multiple essential replicons and a viable distributed genome to form ultimately. In the novel genome, one ER retains the chromosome-like origin of replication and centrosome, and the other the plasmidic counterparts. The novel ERs differ from the chromosome and plasmid that gathered in the progenitor host at the onset. They thus constitute neo-chromosomes that carry divergent maintenance machineries and can cohabit and function in the same cell. Depending on the number of cell cycles spent as co-integrate, the level of genome reorganization, the acquisition of genetic material and the environmental selective pressure acting upon the host, the final essential replicons may exhibit diverse modalities of genome integration (Figure 6).

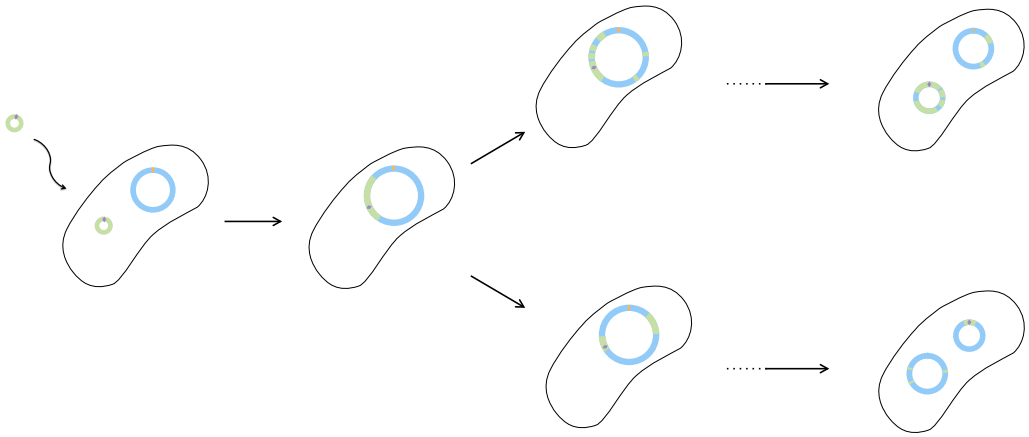

Figure 6. Fusion-Shuffling-Scission model of distributed genome evolution

Origins of replication are represented by diamonds.

The Fusion-Shuffling-Scission model of genome evolution that we propose accounts for the extreme plasticity met in distributed genomes and the eco-phenotypic flexibility of their hosts. Indeed, having a distributed genome appears to extend and accelerate the exploration of the genome evolutionary landscape, producing complex regulation (diCenzo et al., 2018; Galardini et al., 2015; Jiao et al., 2018) and leading to novel eco-phenotypes and species diversification (*e.g.*, Burkholderiaceae and Vibrionaceae). Furthermore, this model may explain the observed separation of the replicons according to taxonomy. Chromosomes and plasmids thus appear as extremes on a continuum of a lineage-specific genetic material.

MATERIALS AND METHODS

To understand the relationships between the chromosomal and plasmidic replicons, we focused on the distribution of Inheritance System (IS) genes for each replicon and built networks linking the replicons given their IS functional orthologues (Fig. 2).

Retrieval of IS functional homologues

A sample of proteins involved in the replication and segregation of bacterial replicons and of the bacterial cell cycle was constructed using datasets available from the ACLAME (Leplae et al., 2010) and KEGG (Kanehisa et al., 2012) databases. Gene ontologies for “replication”, “partition”, “dimer resolution”, and “genome maintenance” (Table 11) were used to select related ACLAME plasmid protein families (Table 1) using a semi-automated procedure.

Table 11. Gene ontologies related to plasmid ISs used to select groups of orthologous proteins from the ACLAME database

PROCESS	ONTOLOGY	DESCRIPTION
Replication	*go:0006270*	DNA replication initiation
	phi:0000268	plasmid vegetative DNA replication
	go:0003896	DNA primase activity
	go:0003887	DNA-directed DNA polymerase activity
	go:0045020	error-prone DNA repair
	go:0006260	DNA replication
	phi:0000114	DNA helicase activity
	go:0006281	DNA repair
	phi:0000196	plasmid copy number control
Partition	*go:0003677*	DNA binding
	575	plasmid partitioning protein family ParB/Spo0J
	go:0015616	DNA translocase activity
	576	plasmid partitioning protein family ParM
	go:0000146	microfilament motor activity
	go:0007059	chromosome segregation
	go:0015616	DNA translocase activity
	go:0007059	chromosome segregation
	go:0016887	ATPase activity
	go:0030541	plasmid partitioning
	go:0051302	regulation of cell division
	phi:0000196	plasmid copy number control
Dimer resolution	*phi:0000134*	site specific DNA excision
	phi:0000144	serine based recombinase activity
	phi : 0000131	site specific DNA recombinaison
	phi : 0000143	Tyrosine-based recombinase activity
	phi : 0000304	plasmid dimer resolution
	go : 0015616	DNA translocase activity
	phi:0000136	transpositional recombination
Maintenance	*go : 0016740*	transferase activity
	phi : 0000262	toxin
	phi:0000322	PSK
	547	TA family parDE
	544	TA family epsilon zeta
	go:0009008	DNA methyltransferase activity
	phi : 0000264	nucleoid associated protein
	go : 0006276	plasmid maintenance

KEGG orthology groups were selected following the KEGG BRITE hierarchical classification (Table 2). Then, the proteins belonging to the relevant 92 ACLAME protein families and 71 KEGG orthology groups (3,847 and 43,757 proteins, respectively) were retrieved and pooled. Using this query set amounting to a total of

549 47,604 proteins, we performed a *blastp* search of the 6,903,452 protein sequences
550 available from the 5,125 complete sequences of bacterial replicons downloaded from
551 NCBI Reference Sequence database (RefSeq) (Pruitt et al., 2007) on 30/11/2012. We
552 identified 358,624 putative homologues using BLAST default parameters (Camacho et
553 al., 2009) and a 10^{-5} significance cut-off value. We chose this *E*-value threshold to
554 enable the capture of similarities between chromosome and plasmid proteins whilst
555 minimizing the production of false positives, *i.e.*, proteins in a given cluster exhibiting
556 small *E*-values despite not being functionally homologous. Using RefSeq ensured the
557 annotation consistency of the genomes included in our dataset.

558 **Clustering of IS functional homologues**

559 Using this dataset, we inferred clusters of IS functional homologues by coupling of an
560 *all-versus-all blastp* search using a 10^{-2} *E*-value threshold and a TRIBE-MCL (Enright et
561 al., 2002) clustering procedure. As input to TRIBE-MCL, we used the matrix of log
562 transformed *E*-value, $d(p_i, p_j) = -\log_{10}\left(e_{value}(p_i, p_j)\right)$, obtained from the comparisons
563 of all possible protein pairs. Using a granularity value of 4.0 (see below), we organized
564 the 358,624 IS homologues into 7013 clusters, each comprising from a single to 1990
565 proteins (Figure 3). We annotated IS homologues according to their best match (BLAST
566 hit with the lowest *E*-value) among the proteins of the query set, *i.e.*, according to one of
567 the 117 functions of the query set (71 from KEGG and 46 from ACLAME). Then, we
568 named the clusters of functional homologues using the most frequent annotation among
569 the proteins in the cluster. We used the number of protein annotations in a cluster to
570 determine the cluster quality, a single annotation being optimal. To select the best
571 granularity and to estimate the consistency of the clusters in terms of functional
572 homologues, we computed the weighted Biological Homogeneity Index (*wBHI*,

modified from the *BHI* (Datta and Datta, 2006), each cluster being weighted by its size) and the Conservation Consistency Measure (*CCM*, similar to the *BHI* but using the functional domains of the proteins to define the reference classes), which both take into account the size distribution of the clusters (See next paragraph for details on index calculation). The former gives an estimation of the overall consistency of clusters annotations according to the protein annotations whereas the latter gives an estimation of cluster homogeneity according to the protein domains identified beforehand. To build the sets of functional domains, we performed an *hmmscan* (Finn et al., 2011) procedure against the Pfam database (Finn et al., 2016) of each of the 358,624 putative IS homologues. We annotated each protein according to the domain match(es) with *E*-value $< 10^{-5}$ (individual *E*-value of the domain) and *c*-*E*-value $< 10^{-5}$ (conditional *E*- value that measures the statistical significance of each domain). If two domains overlapped, we only considered the domain exhibiting the smallest *E*-value. We estimated *wBHI* and *CCM* indices for the clustering of the IS homologues and compared with values obtained for random clusters simulated according to the cluster size distribution of the IS proteins, irrespective of their length or function. For each of the clustering obtained for different granularities, we constructed a random clustering following the original cluster size distribution (assessed with a χ^2 test) and composed with simulated proteins according to the distributions of the type and number of functional domains of the data collected from the 358,624 IS homologues. Overall, the clusters obtained using a granularity of 4.0 with the TRIBE-MCL algorithm appeared to be homogenous in terms of proteins similarities toward their best BLAST hits and their functional domain distributions (see below).

Evaluation of the clustering procedures

In order to select the best granularity and to estimate the consistency of the clusters in

terms of functional homologs, we computed the *weighted Biological Homogeneity Index* (*wBHI*) and the *Conservation Consistency Measure* (*CCM*). The former gives an estimate of the overall consistency of clusters annotations according to the protein annotations whereas the latter gives an estimate of cluster homogeneity according to protein domains identified beforehand. Although close to the *Biological Homogeneity Index* (*BHI*) introduced by Datta and Datta (2006), both these indices take into account the size distribution of the clusters.

The *BHI* was originally introduced to measure the biological homogeneity of clusters according to reference classes to evaluate clusters obtained with microarray data (Datta and Datta, 2006). Given a clustering $C=\{C_1,...,C_k\}$ of k clusters with n_i the size of the cluster C_i, a set of m proteins $P=\{P_1,...,P_m\}$ and a set r of reference classes R where each class R_i could be linked to the m proteins, the BHI is defined as:

$$BHI = \frac{1}{k}\sum_{i=0}^{i<k} c_i$$

where c_i is defined as:

$$c_i = \frac{1}{\left(n_i(n_i-1)\right)}\sum_{P_i,P_j \in C_i} d\left(P_i,P_j\right)$$

where $d(P_i,P_j)=1$ if P_i and P_j share at least one common reference class, and $d(P_i,P_j)=0$ otherwise. The reference classes here are the annotations defined according to the protein best BLAST hit. The *BHI* is thus an easy-to-interpret measure, which value is maximal when, for all clusters, all the proteins in a cluster share at least one annotation.

The *wBHI* is a modification of the *BHI*, where each cluster is weighted by its size m. Following the previous notation scheme, the *wBHI* is defined as:

$$wBHI = \frac{1}{m}\sum_{i=0}^{i<k} 2.c_i.n_i$$

The *CCM* is similar to the *BHI* but the functional domains of the proteins are used to define the reference classes. The distance between the proteins is here computed as the Jaccard distance between the functional domain sets of the proteins. Every protein P_i can be described as a vector of functional domains, $D_{Pi} = \{d_1,...,d_x\}$. The Jaccard distance between the two sets of domains $d_2(P_i,P_j)$ can be defined as:

$$d_2(P_1, P_2) = 1 - \frac{\left|D_{P_1} \cap D_{P_2}\right|}{\left|D_{P_1} \cup D_{P_2}\right|}$$

where D_{P_1} and D_{P_2} are the clans or domains (when no clan could be assigned) identified in P_1 and P_2 respectively. For a given cluster C_i, the *CCM* is calculated as:

$$CCM = \frac{1}{m}\sum_{i=0}^{i<k} 2.c'_i.n_i$$

where c'_i is defined as:

$$c'_i = \frac{1}{\left(n_i(n_i-1)\right)}\sum_{P_i,P_j \in C_i} d_2(P_i, P_j)$$

Clusters which proteins have similar domains result in a *CCM* value close to 0, whereas a *CCM* value close to 1 indicates that the clusters hold proteins with little domain overlap.

Choice of the clustering granularity

We tested several levels of granularity to optimize the TRIBE-MCL clustering and obtain the most informative IS clustering in terms of functional linkage. Too low a granularity would produce large clusters containing multiple functional families. In turn, increasing the granularity results in the tightening of the cluster. A high granularity tends to split clusters harboring different protein subfamilies (*e.g.,* a cluster composed of proteins from the tyrosine recombinase superfamily) and to produce multiple clusters of proteins belonging to a single function family according to their level of sequence

dissimilarity. Furthermore, too high a granularity would result in the formation of numerous single protein clusters, and would dramatically increase the computation times of the following analyses. A granularity level of 4.0 constituted a good compromise (Figure 8). Values of *CCM* and *BHI* are slightly improved compared to granularities of 2.0 and 3.0, and the high but still workable number of clusters is expected to prevent the formation of clusters mingling distinct protein subfamilies.

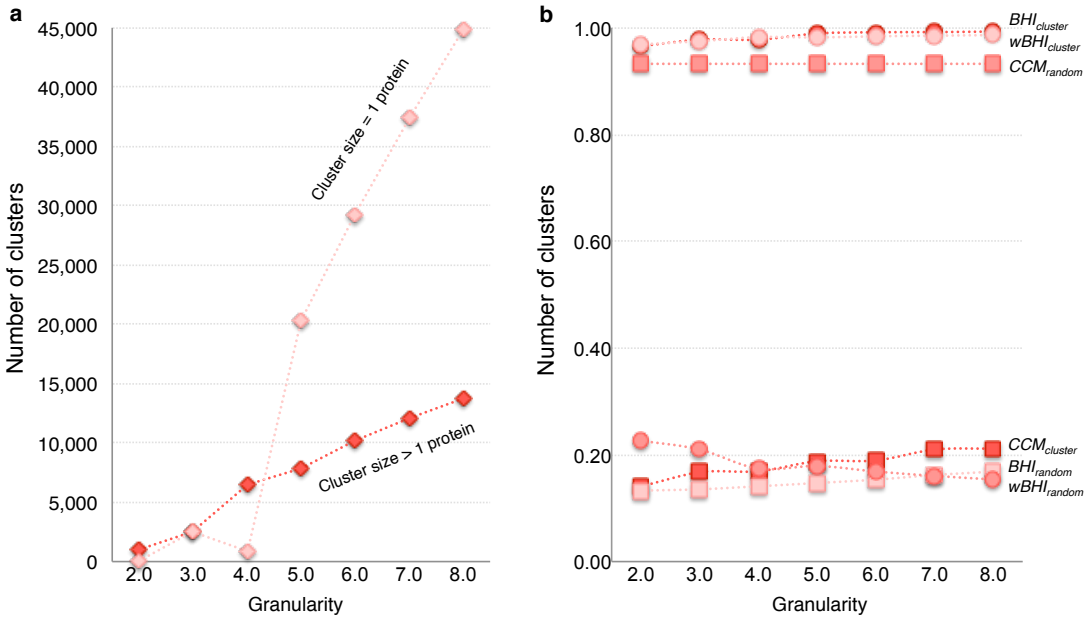

Figure 8. Influence of granularity on the clustering

(a) Number of clusters with more than one protein (dark diamonds) or clusters holding a single protein (pale diamonds). (b) *BHI* (dark), *wBHI* (pale) and *CCM* (medium) scores obtained with random clusters (squares) and normal clusters (circles), respectively.

Assessment of the homogeneity of IS functional homologues

The homogeneity towards the functions of the proteins in the query set relied on the assumption that the first BLAST cut-off (10^{-5} *E*-value) was stringent enough to capture only functional homologues to the query proteins. Potential bias might nevertheless arise from query proteins possessing a supplementary functional domain unrelated to the IS role, or from the selection of proteins belonging to the same superfamily but differing in

function. To address these issues, we calculated the functional vectors associated to each KEGG group or ACLAME family of the query set, as well as those for all obtained clusters. For a protein P_i, we defined the associated functional vector with respect to its set of identified domains D_{P_i} and to the set of all identified domains $D=\{d_1,...,d_X\}$ as:

$$v_{P_i} = \left(n_{d_1}^{P_i}, \dots, n_{d_x}^{P_i}\right)$$

where $n_{d_i}^{P_i}$ is the number of time d_i is found in D_{P_i}. The functional vector associated to a given cluster of proteins C_i could then be defined as:

$$v_{C_i} = \left(n_{d_1}^{C_i}, \dots, n_{d_x}^{C_i}\right)$$

where $n_{d_i}^{C_i}$ is defined as:

$$n_{d_i}^{C_i} = \frac{1}{|C_i|} \sum_{P_i \in C_i} n_{d_x}^{P_j}$$

For each cluster C_0, the cosine distance between its associated vector v_{C_0} and the associated vector v_{C_a} of the corresponding KEGG group or ACLAME family annotations C_a was then computed as:

$$d_{cosine}(v_{C_a}, v_{C_0}) = 1 - \frac{\sum_{i=1}^{X} n_{d_i}^{C_0} . n_{d_i}^{C_a}}{\sqrt{\sum_{i=1}^{X} n_{d_i}^{C_0}{}^2} \cdot \sqrt{\sum_{i=1}^{X} n_{d_i}^{C_a}{}^2}}$$

For each cluster C_0, the cosine distance between its associated vector v_{C_0} and the associated vector v_{C_a} of the corresponding KEGG group or ACLAME family annotations C_a was then computed as:

$$d_{cosine}(v_{C_a}, v_{C_0}) = 1 - \frac{\sum_{i=1}^{X} n_{d_i}^{C_0} . n_{d_i}^{C_a}}{\sqrt{\sum_{i=1}^{X} n_{d_i}^{C_0}{}^2} \cdot \sqrt{\sum_{i=1}^{X} n_{d_i}^{C_a}{}^2}}$$

The $d_{cosine}(v_{C_a}, v_{C_0})$ values were compared with those obtained using random clusters C_r of the same size than C_0. For each C_0 and its corresponding C_a, 200 random clusters and their associated distances $d_{cosine}(v_{C_a}, v_{C_r})$, from which the corresponding empirical

distribution D_e was constructed, were computed. C_0 is then considered as noise if $d_{cosine}(v_{C_a}, v_{C_0}) \notin Q_{10\%}^{D_e}$ where $Q_{10\%}^{D_e}$ is the 0.1-quantile of D_e.

Unsupervised analyses of the replicon space

We represented the bacterial replicons (Supplementary Table 1) as vectors according to their content in IS genes. The number of IS protein clusters retained for the analysis determined the vector dimension and the number of proteins in a replicon assigned to each cluster gave the value of each vector component. We built matrices $P = \begin{bmatrix} p_{1,1} & \cdots & p_{1,m} \\ \vdots & \ddots & \vdots \\ p_{n,1} & \cdots & p_{n,m} \end{bmatrix}$, where n is the number of replicons, m the number of protein clusters, and $p_{i,j}$ the number of proteins of the j^{th} cluster encoded by a gene present on the i^{th} replicon. We constructed several datasets to explore both the replicon type and the host taxonomy effects on the separation of the replicons in the analyses (Table 12).

Table 12. Reference classes used in the evaluation of the replicon IS protein-based unsupervised clustering solutions

EVALUATED SEPARATION	ENSEMBLE	NORMALIZED ENSEMBLE [a]
Chromosomes *vs.* Plasmids	$\left\{R^{\{chromosome\}}, R^{\{plasmid\}}\right\}$	$\left\{\overline{Kl}_{genus}^{R^{\{chromosome\}}}, \overline{Kl}_{genus}^{R^{\{plasmid\}}}\right\}$
Chromosomes *per* host phylum	$Kl_{phylum}^{chromosome}$	$\overline{Kl}_{genus}^{K} \mid K \in Kl_{phylum}^{chromosome}$
Chromosomes *per* host class	$Kl_{class}^{chromosome}$	$\overline{Kl}_{genus}^{K} \mid K \in Kl_{class}^{chromosome}$
Plasmids *per* host phylum	$Kl_{phylum}^{plasmid}$	$\overline{Kl}_{genus}^{K} \mid K \in Kl_{phylum}^{plasmid}$
Plasmids *per* host class	$Kl_{class}^{plasmid}$	$\overline{Kl}_{genus}^{K} \mid K \in Kl_{class}^{plasmid}$

[a] Normalisation according to host genus

The taxonomic representation bias was taken into account by normalizing the data with

682 regard to the host genus: a consensus vector was built for each bacterial genus present in
683 the datasets. The value of each vector attribute was calculated as the mean of the
684 attribute values in the vectors of the replicons that belong to the same bacterial genus.
685 As a first approach, we transformed data into bipartite graphs whose vertices are the
686 replicons and the proteins clusters. The graphs were spatialized using the force-directed
687 layout algorithm ForceAtlas2 (Jacomy et al., 2014) implemented in Gephi (Bastian et al.,
688 2009). Bipartite graphs are a powerful way of representing the data by naturally drawing
689 the links between the replicons while enabling the detailed analysis of the IS cluster-
690 based connections of each replicon by applying forces to each node with regard to its
691 connecting edges. To investigate further the IS-based relationships of the replicons, we
692 applied the community structure detection algorithm INFOMAP (Rosvall and
693 Bergstrom, 2008) using the *igraph* python library (Csardi and Nepusz, 2006). We also
694 performed a WARD hierarchical clustering (Johnson, 1967) after a dimension reduction
695 of the data using a Principal Component Analysis (Hotelling, 1933). To select an
696 optimal number of principal components, we relied on the measurements of the cluster
697 stabilities using a *stability criterion* (Hennig, 2007) and retained the first 30 principal
698 components (57% of the total variance). For consistency purpose, the number of clusters
699 in the WARD analysis was chosen to match that obtained with the INFOMAP
700 procedure. The number of clusters used was assessed by the stability index by Fang and
701 Wang (2012) (Table 3). The quality of the projection and clustering results were
702 confirmed using the V-measure indices (Rosenberg and Hirschberg, 2007) (*homogeneity*,
703 *completeness*, *V-measure*) as external cluster evaluation measures (Table 3). The
704 *homogeneity* indicates how uniform clusters are towards a class of reference. The
705 *completeness* indicates whether reference classes are embedded within clusters. The *V-*
706 *measure* is the harmonic mean between these two indices and indicates the quality of a

clustering solution relative to the classes of reference. These three indices vary between 0 and 1, with values closest to 1 reflecting the good quality of the clustering solution. The type of replicons (*i.e.,* plasmid or chromosome) and the taxonomic affiliation (phylum or class) for chromosomes or plasmids were used as references classes (Table 12). Additionally, the *stability criterion* (Hennig, 2007) of individual clusters, weighted by their size, for a given clustering result was evaluated using the bootstrapping of the original dataset as re-sampling scheme. Individual Jaccard coefficient for each replicon were computed as the number of times that a given replicon of a cluster in a clustering solution is also present in the closest cluster in the resampled datasets.

Functional characterization of the replicons and genomes

In order to characterize the functional bias of the replicons, 117 IS functionalities (46 from ACLAME and 71 from KEGG) were considered. When equivalent in plasmids and chromosomes, functions from ACLAME and KEGG databases were considered to be distinct. A $n*m$ matrix $F = \begin{bmatrix} f_{1,1} & \cdots & f_{1,m} \\ \vdots & \ddots & \vdots \\ f_{n,1} & \cdots & f_{n,m} \end{bmatrix}$ with n the number of replicons and m the number of IS functionalities, was used as input to the projection algorithms. $f_{i,j}$ represents the number of times that genes coding for proteins annotated with the j^{th} function are present on the i^{th} replicon. Several datasets were analysed using PCA dimension reduction of the data followed by WARD hierarchical clustering (Table 3).

Logistic regression analyses

Several reference classes of replicons and complete genomes were considered for comparison (Table 13). Ambiguous, *i.e.*, potentially adapted, plasmids belonging to INFOMAP clusters of plasmid replicons partially composed of SERs and/or chromosomes were removed from the plasmid class. When appropriate, the taxonomic

representation bias was taken into account by normalizing the data with regard to the host genus as before. Logistic regressions (McCullagh and Nelder, 1989) were performed for the 117 IS functions using the R glm package coupled to the python binder rpy2. The computed P_{value} measured the probability of a functionality to be predictive of a given group of replicons/genomes and the *Odd-Ratio* estimated how the functionality occurrence influenced the belonging of a replicon/genome to a given group.

Table 13. Datasets used in the logistic regression analyses

ENSEMBLE OF REPLICONS OR GENOMES	NOTATION	DATASET	DIMENSION[a]
Genus-normalized SERs	E_{SER}	$\bar{V}_{f,genus}^{R\{SER\}}$	(28, 117)
Genus-normalized plasmids	$E_{plasmid}$	$\bar{V}_{f,genus}^{R\{plasmid\}}$	(262, 117)
Genus-normalized chromosomes	$E_{chromosome}$	$\bar{V}_{f,genus}^{R\{chromosome\}}$	(560, 117)

[a] (Number of replicons, number of functions)

Supervised classification of replicons and genomes

In order to identify putative ill-defined SERs and chromosomes amongst plasmids, we performed supervised classification analyses using random forest procedures (Geurts et al., 2006). We used the IS functionalities as the set of features and the whole sets of chromosomes, plasmids and SER as sets of samples to build four classification studies (Table 7) and detect SER candidates (plasmids *vs.* SERs) and chromosome candidates (chromosomes *vs.* SERs or chromosomes *vs.* plasmids). Because of the unbalanced sizes of the training classes (SERs *vs.* chromosomes and plasmids), iterative sampling procedures were performed using 1000 random subsets of the largest class, with a size

similar to that of the smallest class. The ensuing results were averaged to build the class probabilities and relative importance of the variables. We also used the whole set of plasmids when compared to SERs, to identify more robust SER candidates. The discarding of plasmids in the iterative procedure increases the classifier sensitivity while reducing the rate of false negatives by including more plasmid-annotated putative true SERs, whereas it decreases the classifier precision while increasing the rate of false positives. The ExtraTreeClassifier (a classifier similar to Random Forest) class from the Scikit-learn python library (Pedregosa et al., 2011) was used to perform the classifications, with *K=1000*, *max_feat=sqrt(number of variables)* and *min_split=1*. For each run, the *feature_importances* and *estimate_proba* functions were used to compute, respectively, the relative contribution of the input variables and the class probabilities of replicons/genomes. The statistical probability of a replicon/genome belonging to a class was calculated as the average predicted class of the trees in the forest. The relative contribution of the input variables was estimated according to Breiman (2001). The choices of the number of trees in the forest *K*, the number of variables selected for each split *max_feat*, and the minimum number of samples required to split an internal node *min_split* were cross-validated using a *Leave-One-Out* scheme. The performance of the *Extremely-randomized-trees* classification procedures was assessed using a stratified 10-fold cross-validation procedure following Han *et al.* (2012), and the out-of-bag estimate (OOB score) (Izzenman, 2008; Pedregosa et al., 2011) computed using the *oob_score* function of Scikit-learn python library.

Data availability

The data supporting the findings of this study are available within the Article and its Supplementary Information or are available from the authors.

REFERENCES

Acosta-Cruz E, Wisniewski-Dyé F, Rouy Z, Barbe V, Valdés M, Mavingui P. 2012. Insights into the 1.59-Mbp largest plasmid of *Azospirillum brasilense* CBG497. *Archives in Microbiology*. **194**:725-736. doi: 10.1007/s00203-012-0805-2.

Alav I, Sutton JM, Rahman KM. 2018. Role of bacterial efflux pumps in biofilm formation. *Journal of Antimicrobial Chemotherapy*. **73**:2003-2020. doi: 10.1093/jac/dky042.

Anes J, McCusker MP, Fanning S, Martins M. 2015. The ins and outs of RND efflux pumps in Escherichia coli. *Frontiers in Microbiology*. **6**:587. doi: 10.3389/fmicb.2015.00587.

Baek JH, Chattoraj DK. 2014. Chromosome I controls chromosome II replication in *Vibrio cholerae*. *PLOS Genetics*. **10**:e1004184. doi: 10.1371/journal.pgen.1004184.

Barbe V, Bouzon M, Mangenot S, Badet B, Poulain J, Segurens B, Vallenet D, Marlière P, Weissenbach J. 2011. Complete genome sequence of *Streptomyces cattleya* NRRL 8057, a producer of antibiotics and fluorometabolites. *Journal of Bacteriology*. **193**:5055-5056. doi: 10.1128/JB.05583-11.

Bastian M, Heymann S, Jacomy M. 2009. Gephi: An open source software for exploring and manipulating networks. *Third International AAAI Conference on Weblogs and Social Media, San Jose Mc Enery Convention Center, May 17, 2009 - May 20, 2009: AAAI Publications*.

Blanco-Ordóñez H, Oliva-García JJ, Pérez-Mendoza D, Soto MJ, Olivares J, Sanjúan J, Nogales J. 2010. pSymA-dependent mobilization of the *Sinorhizobium meliloti* pSymB megaplasmid. *Journal of Bacteriology*. **192**:6309-6312. doi:

796 10.1128/JB.00549-10.
797 Breiman L. 2001. Random forests. *Machine Learning*. **45**:5-32. doi:
798 10.1023/A:1010933404324.
799 Brom S, García-de los Santos A, Cervantes L, Palacios R, Romero D. 2000. In
800 *Rhizobium etli* symbiotic plasmid transfer, nodulation competitivity and cellular
801 growth require interaction among different replicons. *Plasmid*. **44**:34-43. doi:
802 10.1006/plas.2000.1469
803 Camacho CJ, Coulouris G, Avagyan V, Ma N, Papdopoulos J, Bealer K, Madden TL.
804 2009. BLAST+: architecture and applications. *BMC Bioinformatics*. **10**:421. doi:
805 10.1186/1471-2105-10-421.
806 Casjens SR. 1998. The diverse and dynamic structure of bacterial genomes. *Annual*
807 *review of genetics*. **32**:339-377. doi: 10.1146/annurev.genet.32.1.339.
808 Cervantes L, Bustos P, Girard L, Santamaría RI, Dávila G, Vinuesa P, Romero D, Brom
809 S. 2011. The conjugative plasmid of a bean-nodulating *Sinorhizobium fredii*
810 strain is assembled from sequences of two *Rhizobium* plasmids and the
811 chromosome of a *Sinorhizobium* strain. *BMC microbiology*. **11**:149. doi:
812 10.1186/1471-2180-11-149.
813 Chen Y, Milam SL, Erickson HP. 2012. SulA inhibits assembly of FtsZ by a simple
814 sequestration mechanism. *Biochemistry.* **51**:3100–3109. doi: 10.1021/bi201669d.
815 Chodavarapu S, Jones AD, Feig M, Kaguni JM. 2016. DnaC traps DnaB as an open ring
816 and remodels the domain that binds primase. *Nucleic Acids Research*. **44**:210-
817 220. doi: 10.1093/nar/gkv961.
818 Csárdi G, Nepusz T. 2006. The igraph software package for complex network research.
819 *InterJournal, Complex Systems*.1695.
820 Datta S, Datta S. 2006. Methods for evaluating clustering algorithms for gene expression

data using a reference set of functional classes. *BMC Bioinformatics*. **7**:397. doi: 10.1186/1471-2105-7-397.

De Nisco NJ, Abo RP, Wu CM, Penterman J, Walker GC. 2014. Global analysis of cell cycle gene expression of the legume symbiont *Sinorhizobium meliloti*. *Proceedings of the National Academy of Sciences of the United States of America*. **111**:3217-3224. doi: 10.1073/pnas.1400421111.

Deghelt M, Mullier C, Sternon JF, Francis N, Laloux G, Dotreppe D, Van der Henst C, Jacobs-Wagner C, Letesson JJ, De Bolle X. 2014. G1-arrested newborn cells are the predominant infectious form of the pathogen *Brucella abortus*. *Nature communications*. **5**:4366. doi: 10.1038/ncomms5366.

Demarre G, Galli E, Muresan L, Paly E, David A, Possoz C, Barre F-X. 2014. Differential management of the replication terminus regions of the two *Vibrio cholerae* chromosomes during cell division. *PLOS Genetics*. **10**:e1004557. doi: 10.1371/journal.pgen.1004557.

diCenzo G, Milunovic B, Cheng J, Finan TM. 2013. The tRNAarg gene and *engA* are essential genes on the 1.7-Mb pSymB megaplasmid of *Sinorhizobium meliloti* and were translocated together from the chromosome in an ancestral strain. *Journal of Bacteriology*. **195**:202-212. doi: 10.1128/JB.01758-12.

diCenzo GC, Finan TM. 2017. The divided bacterial genome: structure, function, and evolution. *Microbiology and Molecular Biology Reviews*. **81**:e00019-00017. doi: 10.1128/MMBR.00019-17.

diCenzo GC, MacLean AM, Milunovic B, Golding GB, Finan TM. 2014. Examination of prokaryotic nultipartite genome evolution through experimental genome reduction. *PLOS Genetics*. **10**:e1004742. doi: 10.1371/journal.pgen.1004742.

diCenzo GC, Wellappili D, Golding GB, Finan TM. 2018. Inter-replicon gene flow

846 contributes to transcriptional integration in the *Sinorhizobium meliloti*
847 multipartite genome. *G3 (Bethesda)*. **8**:1711-1720. doi: 10.1534/g3.117.300405.
848 Dillon SC, Dorman CJ. 2010. Bacterial nucleoid-associated proteins, nucleoid structure
849 and gene expression. *Nat Rev Microbiol*. **8**:185-195. doi: 10.1038/nrmicro2261.
850 Drevinek P, Baldwin A, Dowson CG, Mahenthiralingam E. 2008. Diversity of the *parB*
851 and *repA* genes of the *Burkholderia cepacia* complex and their utility for rapid
852 identification of *Burkholderia cenocepacia*. *BMC microbiology*. **8**:44. doi:
853 10.1186/1471-2180-8-44.
854 Du D, Wang-Kan X, Neuberger A, van Veen HW, Pos KM, Piddock LJV, Luisi BF.
855 2018. Multidrug efflux pumps: structure, function and regulation. *Nature Review*
856 *in Microbiology*. **16**:523-539. doi: 10.1038/s41579-018-0048-6.
857 Dubarry N, Pasta F, Lane D. 2006. ParABS systems of the four replicons of
858 *Burkholderia cenocepacia*: new chromosome centromeres confer partition
859 specificity. *Journal of Bacteriology*. **188**:1489-1496. doi:
860 10.1128/JB.188.4.1489-1496.2006.
861 Egan ES, Lobner-Olesen A, Waldor MK. 2004. Synchronous replication initiation of the
862 two *Vibrio cholerae* chromosomes. *Current Biology*. **14**:R501-502. doi:
863 10.1016/j.cub.2004.06.036.
864 Egan ES, Waldor MK. 2003. Distinct replication requirements for the two *Vibrio*
865 *cholerae* chromosomes. *Cell*. **114**:521-530. doi: 10.1016/s0092-8674(03)00611-
866 1.
867 Enright AJ, Dongen S, Ouzounis C. 2002. An efficient algorithm for large-scale
868 detection of protein families. *Nucleic Acids Research*. **30**:1575-1584. doi:
869 10.1093/nar/30.7.1575.
870 Fang Y, Wang J. 2012. Selection of the number of clusters via the bootstrap method.

871 *Computational Statistics & Data Analysis*. **56**:468-477. doi:
872 10.1016/j.csda.2011.09.003.
873 Fiebig A, Keren K, Theriot JA. 2006. Fine-scale time-lapse analysis of the biphasic,
874 dynamic behaviour of the two *Vibrio cholerae* chromosomes. *Molecular*
875 *Microbiology*. **60**:1164-1178. doi: 10.1111/j.1365-2958.2006.05175.x.
876 Finn RD, Clements J, Eddy SR. 2011. HMMER web server: interactive sequence
877 similarity searching. *Nucleic Acids Research*. **39**:W29-37. doi:
878 10.1093/nar/gkr367.
879 Finn RD, Coggill P, Eberhardt RY, Eddy SR, Mistry J, Mitchell AL, Potter SC, Punta
880 M, Qureshi M, Sangrador-Vegas A, Salazar GA, Tate J, Bateman A. 2016. The
881 Pfam protein families database: towards a more sustainable future. *Nucleic Acids*
882 *Research*. **44**:D279-285. doi: 10.1093/nar/gkv1344.
883 Frage B, Dohlemann J, Robledo M, Lucena D, Sobetzko P, Graumann PL, Becker A.
884 2016. Spatiotemporal choreography of chromosome and megaplasmids in the
885 *Sinorhizobium meliloti* cell cycle. *Molecular Microbiology*. **100**:808-823. doi:
886 10.1111/mmi.13351.
887 Galardini M, Mengoni A, Brilli M, Pini F, Fioravanti A, Lucas S, Lapidus A, Cheng JF,
888 Goodwin L, Pitluck S, Land M, Hauser L, Woyke T, Mikhailova N, Ivanova N,
889 Daligault H, Bruce D, Detter C, Tapia R, Han C, Teshima H, Mocali S,
890 Bazzicalupo M, Biondi EG. 2011. Exploring the symbiotic pangenome of the
891 nitrogen-fixing bacterium *Sinorhizobium meliloti*. *BMC Genomics*. **12**:235. doi:
892 10.1186/1471-2164-12-235.
893 Galardini M, Pini F, Bazzicalupo M, Biondi G, Mengoni A. 2013. Replicon-dependent
894 bacterial genome evolution: the case of *Sinorhizobium meliloti*. *Genome Biology*
895 *and Evolution*. **5**:542-558. doi: 10.1093/gbe/evt027.

Galardini M, Brilli M, Spini G, Rossi M, Roncaglia B, Bani A, Chiancianesi M, Moretto M, Engelen K, Bacci G, Pini F, Biondi EG, Bazzicalupo M, Mengoni A. 2015. Evolution of Intra-specific Regulatory Networks in a Multipartite Bacterial Genome. *PLoS Computational Biology* **11**:e1004478. doi: 10.1371/journal.pcbi.1004478.

Galli E, Poidevin M, Le Bars R, Desfontaines JM, Muresan L, Paly E, Yamaichi Y, Barre FX. 2016. Cell division licensing in the multi-chromosomal *Vibrio cholerae* bacterium. *Nat Microbiology*. **1**:16094. doi: 10.1038/nmicrobiol.2016.94.

Gerding MA, Chao MC, Davis BM, Waldor MK. 2015. Molecular dissection of the essential features of the origin of replication of the second *Vibrio cholerae* chromosome. *MBio*. **6**:e00973. doi: 10.1128/mBio.00973-15.

Geurts P, Ernst D, Wehenkel L. 2006. Extremely randomized trees. *Machine Learning*. **63**:3-42. doi: 10.1007/s10994-006-6226-1.

Guo FB, Ning LW, Huang J, Lin H, Zhang HX. 2010. Chromosome translocation and its consequence in the genome of *Burkholderia cenocepacia* AU-1054. *Biochemical and Bophysical Research Communications*. **403**:375-379. doi: 10.1016/j.bbrc.2010.11.039.

Guo X, Flores M, Mavingui P, Fuentes SI, Hernandez G, Davila G, Palacios R. 2003. Natural genomic design in *Sinorhizobium meliloti*: novel genomic architectures. *Genome Research*. **13**:1810-1817. doi: 10.1101/gr.1260903.

Hall JPJ, Brockhurst MA, Dytham C, Harrison E. 2017. The evolution of plasmid stability: Are infectious transmission and compensatory evolution competing evolutionary trajectories? *Plasmid*. **91**:90-95. doi: 10.1016/j.plasmid.2017.04.003.

921 Han J, Kamber M, Pei J. 2012. Data Mining: Concepts and Techniques, Third Edition:
922 Morgan kaufmann, Elsevier.
923 Harrison PW, Lower RP, Kim NK, Young JPW. 2010. Introducing the bacterial
924 'chromid': not a chromosome, not a plasmid. *Trends in Microbiology*. **18**:141-
925 148. doi: 10.1016/j.tim.2009.12.010.
926 Hennig C. 2007. Cluster-wise assessment of cluster stability. *Computational Statistics &*
927 *Data Analysis*. **52**:258-271. doi: 10.1016/j.csda.2006.11.025.
928 Hotelling H. 1933. Analysis of a complex of statistical variables into principal
929 components. *Journal of Educational Psychology*. **24**:417. doi:
930 10.1037/h0071325.
931 Izenman AJ. 2008. Modern multivariate statistical techniques: regression, classification,
932 and manifold learning: Springer-Verlag, New York Inc.
933 Jacomy M, Venturini T, Heymann S, Bastian M. 2014. ForceAtlas2, a continuous graph
934 layout algorithm for handy network visualization designed for the Gephi
935 software. *PLoS One*. **9**:e98679. doi: 10.1371/journal.pone.0098679.
936 Jiao J, Ni M, Zhang B, Zhang Z, Young JPW, Chan TF, Chen WX, Lam HM, Tian CF.
937 2018. Coordinated regulation of core and accessory genes in the multipartite
938 genome of Sinorhizobium fredii. *PLoS Genet*ics **14**:e1007428. doi:
939 10.1371/journal.pgen.1007428.
940 Johnson SC. 1967. Hierarchical clustering schemes. *Psychometrika*. **32**:241-254.
941 Kahng LS, Shapiro L. 2003. Polar localization of replicon origins in the multipartite
942 genomes of *Agrobacterium tumefaciens* and *Sinorhizobium meliloti*. *Journal of*
943 *Bacteriology*. **185**:3384-3391. doi: 10.1128/jb.185.11.3384-3391.2003.
944 Kanehisa M, Goto S, Sato Y, Furumichi M, Tanabe M. 2012. KEGG for integration and
945 interpretation of large-scale molecular data sets. *Nucleic Acids Research*.

946 **40**:D109-114. doi: 10.1093/nar/gkr988.
947 Kemter FS, Messerschmidt SJ, Schallopp N, Sobetzko P, Lang E, Bunk B, Sproer C,
948 Teschler JK, Yildiz FH, Overmann J, Waldminghaus T. 2018. Synchronous
949 termination of replication of the two chromosomes is an evolutionary selected
950 feature in Vibrionaceae. *PLOS Genetics*. **14**:e1007251. doi:
951 10.1371/journal.pgen.1007251.
952 Krawiec S, Riley M. 1990. Organization of the bacterial chromosome. *Microbiological*
953 *Reviews*. **54**:502-539.
954 Landeta C, Dávalos A, Cevallos MÁ, Geiger O, Brom S, Romero D. 2011. Plasmids
955 with a chromosome-like role in rhizobia. *Journal of Bacteriology*. **193**:1317-
956 1326. doi: 10.1128/JB.01184-10.
957 Lederberg J. 1998. Plasmid (1952-1997). *Plasmid*. **39**:1-9. doi: 10.1006/plas.1997.1320.
958 Leplae R, Lima-Mendez G, Toussaint A. 2010. ACLAME: a CLAssification of Mobile
959 genetic Elements, update 2010. *Nucleic Acids Research*. **38**:D57-61. doi:
960 10.1093/nar/gkp938.
961 Li Y, Canchaya C, Fang F, Raftis E, Ryan KA, van Pijkeren J-P, van Sinderen D,
962 O'Toole PW. 2007. Distribution of megaplasmids in *Lactobacillus salivarius* and
963 other lactobacilli. *Journal of Bacteriology*. **189**:6128-6139. doi:
964 10.1128/JB.00447-07.
965 Lioy VS, Cournac A, Marbouty M, Duigou S, Mozziconacci J, Espeli O, Boccard F,
966 Koszul R. 2018. Multiscale structuring of the *E. coli* chromosome by nucleoid-
967 associated and condensin proteins. *Cell*. **172**:771-783 e718. doi:
968 10.1016/j.cell.2017.12.027.
969 Liu G, Yong MY, Yurieva M, Srinivasan KG, Liu J, Lim JS, Poidinger M, Wright GD,
970 Zolezzi F, Choi H, Pavelka N, Rancati G. 2015. Gene essentiality is a

quantitative property linked to cellular evolvability. *Cell*. **163**:1388-1399. doi: 10.1016/j.cell.2015.10.069.

Livny J, Yamaichi Y, Waldor MK. 2007. Distribution of centromere-like parS sites in bacteria: insights from comparative genomics. *Journal of Bacteriology*. **189**:8693-8703. doi: 10.1128/JB.01239-07.

Lu C, Nakayasu ES, Zhang LQ, Luo ZQ. 2016. Identification of Fic-1 as an enzyme that inhibits bacterial DNA replication by AMPylating GyrB, promoting filament formation. *Science Signal*. **9**:ra11. doi: 10.1126/scisignal.aad0446.

Mackenzie C, Kaplan S, Choudhary M. 2004. Multiple chromosomes. *In: Miller RV and Day MJ, editors. Microbial Evolution: Gene Establishment, Survival, and Exchange: ASM press, Washington DC*:82-101.

Mackenzie C, Simmons AE, Kaplan S. 1999. Multiple chromosomes in bacteria: the Yin and Yang of *trp* gene localization in *Rhodobacter sphaeroides* 2.4.1. *Genetics*. **153**:525-538.

MacLellan SR, Sibley CD, Finan TM. 2004. Second chromosomes and megaplasmids in bacteria. *In: Funnel BE and Phillips GJ, editors. Plasmid biology: ASM press, Washington DC*:529-542.

MacLellan SR, Zaheer R, Sartor AL, MacLean AM, Finan TM. 2006. Identification of a megaplasmid centromere reveals genetic structural diversity within the repABC family of basic replicons. *Molecular Microbiology*. **59**:1559-1575. doi: 10.1111/j.1365-2958.2005.05040.x.

Maida I, Fondi M, Orlandini V, Emiliani G, Papaleo MC, Perrin E, Fani R. 2014. Origin, duplication and reshuffling of plasmid genes: Insights from *Burkholderia vietnamiensis* G4 genome. *Genomics*. **103**:229-238. doi: 10.1016/j.ygeno.2014.02.004.

McCullagh P, Nelder JA. 1989. Generalized linear models, Second Edition: Chapman & Hall/CRC, London. 532 p.

Medema MH, Trefzer A, Kovalchuk A, van den Berg M, Muller U, Heijne W, Wu L, Alam MT, Ronning CM, Nierman WC, Bovenberg RA, Breitling R, Takano E. 2010. The sequence of a 1.8-mb bacterial linear plasmid reveals a rich evolutionary reservoir of secondary metabolic pathways. *Genome Biology and Evolution*. **2**:212-224. doi: 10.1093/gbe/evq013.

Meier EL, Daitch AK, Yao Q, Bhargava A, Jensen GJ, Goley ED. 2017. FtsEX-mediated regulation of the final stages of cell division reveals morphogenetic plasticity in *Caulobacter crescentus*. *PLoS Genetics* **13**: e1006999. doi: 10.1371/journal.pgen.1006999.

Million-Weaver S, Camps M. 2014. Mechanisms of plasmid segregation: have multicopy plasmids been overlooked? *Plasmid*. **75**:27-36. doi: 10.1016/j.plasmid.2014.07.002.

Murray H, Errington J. 2008. Dynamic control of the DNA replication initiation protein DnaA by Soj/ParA. *Cell*. **135**:74-84. doi: 10.1016/j.cell.2008.07.044.

Naito M, Ogura Y, Itoh T, Shoji M, Okamoto M, Hayashi T, Nakayama K. 2016. The complete genome sequencing of *Prevotella intermedia* strain OMA14 and a subsequent fine-scale, intra-species genomic comparison reveal an unusual amplification of conjugative and mobile transposons and identify a novel *Prevotella*-lineage-specific repeat. *DNA Research*. **23**:11-19. doi: 10.1093/dnares/dsv032.

Ohtani N, Tomita M, Itaya M. 2010. An extreme thermophile, *Thermus thermophilus*, is a polyploid bacterium. *Journal of Bacteriology*. **192**:5499-5505. doi: 10.1128/JB.00662-10.

1021 Passot FM, Calderon V, Fichant G, Lane D, Pasta F. 2012. Centromere binding and
1022 evolution of chromosomal partition systems in the Burkholderiales. *Journal of*
1023 *Bacteriology*. **194**:3426-3436. doi: 10.1128/JB.00041-12.
1024 Pedregosa F, Weiss R, Brucher M. 2011. Scikit-learn : Machine Learning in Python.
1025 *Journal of Machine Learning Research*. **12**:2825-2830.
1026 http://www.jmlr.org/papers/volume12/pedregosa11a/pedregosa11a.pdf.
1027 Petersen J, Frank O, Göker M, Pradella S. 2013. Extrachromosomal, extraordinary and
1028 essential--the plasmids of the *Roseobacter* clade. *Applied Microbiology and*
1029 *Biotechnology*. **97**:2805-2815. doi: 10.1007/s00253-013-4746-8.
1030 Pinto UM, Pappas KM, Winans SC. 2012. The ABCs of plasmid replication and
1031 segregation. *Nature Review in Microbiology*. **10**:755-765. doi:
1032 10.1038/nrmicro2882.
1033 Pruitt KD, Tatusova T, Maglott DR. 2005. NCBI Reference Sequence (RefSeq): a
1034 curated non-redundant sequence database of genomes, transcripts and proteins.
1035 *Nucleic Acids Research*. **33**:D501-504. doi: 10.1093/nar/gki025.
1036 Rasmussen T, Jensen RB, Skovgaard O. 2007. The two chromosomes of *Vibrio cholerae*
1037 are initiated at different time points in the cell cycle. *EMBO Journal*. **26**:3124-
1038 3131. doi: 10.1038/sj.emboj.7601747.
1039 Reyes-Lamothe R, Tran T, Meas D, Lee L, Li AM, Sherratt DJ, Tolmasky ME. 2014.
1040 High-copy bacterial plasmids diffuse in the nucleoid-free space, replicate
1041 stochastically and are randomly partitioned at cell division. *Nucleic Acids*
1042 *Research*. **42**:1042-1051. doi: 10.1093/nar/gkt918.
1043 Rosenberg A, Hirschberg J. 2007. V-Measure: A conditional entropy-based external
1044 cluster evaluation measure. *Proceedings of the 2007 Joint Conference on*
1045 *Empirical Methods in Natural Language Processing and Computational Natural*

Language Learning (EMNLP-CoNLL) p. 410-420. https://www.researchgate.net/publication/221012656_V-Measure_A_Conditional_Entropy-Based_External_Cluster_Evaluation_Measure.

Rosvall M, Bergstrom CT. 2008. Maps of random walks on complex networks reveal community structure. *Proceedings of the National Academy of Sciences of the United States of America*. **105**:1118-1123. doi: 10.1073/pnas.0706851105.

San Millan A, Peña-Miller R, Toll-Riera M, Halbert ZV, McLean aR, Cooper BS, MacLean RC. 2014. Positive selection and compensatory adaptation interact to stabilize non-transmissible plasmids. *Nature communications*. **5**:5208. doi: 10.1038/ncomms6208.

Slater SC, Goldman BS, Goodner B, Setubal JC, Farrand SK, Nester EW, Burr TJ, Banta L, Dickerman AW, Paulsen I, Otten L, Suen G, Welch R, Almeida NF, Arnold F, Burton OT, Du Z, Ewing A, Godsy E, Heisel S, Houmiel KL, Jhaveri J, Lu J, Miller NM, Norton S, Chen Q, Phoolcharoen W, Ohlin V, Ondrusek D, Pride N, Stricklin SL, Sun J, Wheeler C, Wilson L, Zhu H, Wood DW. 2009. Genome sequences of three *Agrobacterium* biovars help elucidate the evolution of multichromosome genomes in bacteria. *Journal of Bacteriology*. **191**:2501-2511. doi: 10.1128/JB.01779-08.

Srivastava P, Fekete RA, Chattoraj DK. 2006. Segregation of the replication terminus of the two *Vibrio cholerae* chromosomes. *Journal of Bacteriology*. **188**:1060-1070. doi: 10.1128/JB.188.3.1060-1070.2006.

Stalder T, Rogers LM, Renfrow C, Yano H, Smith Z, Top EM. 2017. Emerging patterns of plasmid-host coevolution that stabilize antibiotic resistance. *Scientific Reports*. **7**:4853. doi: 10.1038/s41598-017-04662-0.

1071 Stokke C, Waldminghaus T, Skarstad K. 2011. Replication patterns and organization of
1072 replication forks in *Vibrio cholerae*. *Microbiology*. **157**:695-708. doi:
1073 10.1099/mic.0.045112-0.
1074 Sýkora P. 1992. Macroevolution of plasmids: A model for plasmid speciation. *Journal*
1075 *of theoretical biology*. **159**:53-65. doi: 10.1016/s0022-5193(05)80767-2.
1076 Val M-E, Kennedy SP, El Karoui M, Bonné L, Chevalier F, Barre F-X. 2008. FtsK-
1077 dependent dimer resolution on multiple chromosomes in the pathogen *Vibrio*
1078 *cholerae*. *PLOS Genetics*. **4**:e1000201. doi: 10.1371/journal.pgen.1000201.
1079 Val M-E, Kennedy SP, Soler-Bistué AJ, Barbe V, Bouchier C, Ducos-Galand M,
1080 Skovgaard O, Mazel D. 2014. Fuse or die: how to survive the loss of Dam in
1081 *Vibrio cholerae*. *Molecular Microbiology*. **91**:665-678. doi: 10.1111/mmi.12483.
1082 Venkova-Canova T, Chattoraj DK. 2011. Transition from a plasmid to a chromosomal
1083 mode of replication entails additional regulators. *Proceedings of the National*
1084 *Academy of Sciences of the United States of America*. **108**:6199-6204. doi:
1085 10.1073/pnas.1013244108.
1086 Villaseñor T, Brom S, Davalos A, Lozano L, Romero D, Los Santos AG. 2011.
1087 Housekeeping genes essential for pantothenate biosynthesis are plasmid-encoded
1088 in *Rhizobium etli* and *Rhizobium leguminosarum*. *BMC microbiology*. **11**:66. doi:
1089 10.1186/1471-2180-11-66.
1090 Vuilleumier S, Chistoserdova L, Lee MC, Bringel F, Lajus A, Zhou Y, Gourion B,
1091 Barbe V, Chang J, Cruveiller S, Dossat C, Gillett W, Gruffaz C, Haugen E,
1092 Hourcade E, Levy R, Mangenot S, Muller E, Nadalig T, Pagni M, Penny C,
1093 Peyraud R, Robinson DG, Roche D, Rouy Z, Saenampechek C, Salvignol G,
1094 Vallenet D, Wu Z, Marx CJ, Vorholt JA, Olson MV, Kaul R, Weissenbach J,
1095 Medigue C, Lidstrom ME. 2009. *Methylobacterium* genome sequences: a

reference blueprint to investigate microbial metabolism of C1 compounds from natural and industrial sources. *PLoS One*. **4**:e5584. doi: 10.1371/journal.pone.0005584.

Webber MA, Bailey AM, Blair JM, Morgan E, Stevens MP, Hinton JC, Ivens A, Wain J, Piddock LJ. 2009. The global consequence of disruption of the AcrAB-TolC efflux pump in *Salmonella enterica* includes reduced expression of SPI-1 and other attributes required to infect the host. *Journal of Bacteriology*. **191**:4276-4285. doi: 10.1128/JB.00363-09.

Wisniewski-Dyé F, Borziak K, Khalsa-Moyers G, Alexandre G, Sukharnikov LO, Wuichet K, Hurst GB, McDonald WH, Robertson JS, Barbe V, Calteau A, Rouy Z, Mangenot S, Prigent-Combaret C, Normand P, Boyer M, Siguier P, Dessaux Y, Elmerich C, Condemine G, Krishnen G, Kennedy I, Paterson AH, González V, Mavingui P, Zhulin IB. 2011. *Azospirillum* genomes reveal transition of bacteria from aquatic to terrestrial environments. *PLOS Genetics*. **7**:e1002430. doi: 10.1371/journal.pgen.1002430.

Wisniewski-Dyé F, Lozano L, Acosta-Cruz E, Borland S, Drogue B, Prigent-Combaret C, Rouy Z, Barbe V, Mendoza Herrera A, González V, Mavingui P. 2012. Genome sequence of *Azospirillum brasilense* CBG497 and comparative analyses of *Azospirillum* core and accessory genomes provide Insight into niche adaptation. *Genes (Basel)*. **3**:576-602. doi: 10.3390/genes3040576.

Xie G, Johnson SL, Davenport KW, Rajavel M, Waldminghaus T, Detter JC, Chain PS, Sozhamannan S. 2017. Exception to the rule: genomic characterization of naturally occurring unusual *Vibrio cholerae* strains with a single chromosome. *International Journal of Genomics*. **2017**:8724304. doi: 10.1155/2017/8724304.

Yamaichi Y, Fogel MA, McLeod SM, Hui MP, Waldor MK. 2007. Distinct centromere-

like *parS* sites on the two chromosomes of *Vibrio* spp. *Journal of Bacteriology*. **189**:5314-5324. doi: 10.1128/JB.00416-07.

Yamamoto S, Lee K-i, Morita M, Arakawa E, Izumiya H, Ohnishi M. 2018. Single circular chromosome identified from the genome sequence of the *Vibrio cholerae* O1 bv. El Tor Ogawa strain V060002. *Genome Announcements*. **6**. doi: 10.1128/genomeA.00564-18.

Yeoman CJ, Kelly WJ, Rakonjac J, Leahy SC, Altermann E, Attwood GT. 2011. The large episomes of *Butyrivibrio proteoclasticus* B316T have arisen through intragenomic gene shuttling from the chromosome to smaller *Butyrivibrio*-specific plasmids. *Plasmid*. **66**:67-78. doi: 10.1016/j.plasmid.2011.05.002.

SUPPLEMENTARY TABLES

Table 1. Replicon dataset

Table 2. INFOMAP IS protein-based clustering solution of the 4928 replicons

Table 3. PCA + WARD IS protein-based clustering solution of the 4928 replicons

Table 4. PCA + WARD IS function-based clustering solution of the 4928 replicons